

**STUDY OF SIX PHASE POWER
TRANSMISSION NETWORK**

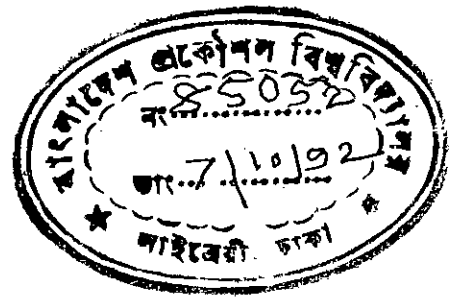
A THESIS

SUBMITTED TO THE DEPARTMENT OF ELECTRICAL AND ELECTRONIC ENGINEERING,
BANGLADESH UNIVERSITY OF ENGINEERING AND TECHNOLOGY IN PARTIAL
FULFILMENT OF THE REQUIREMENTS FOR THE DEGREE OF MASTER OF SCIENCE IN
ENGINEERING (ELECTRICAL AND ELECTRONIC)

BY

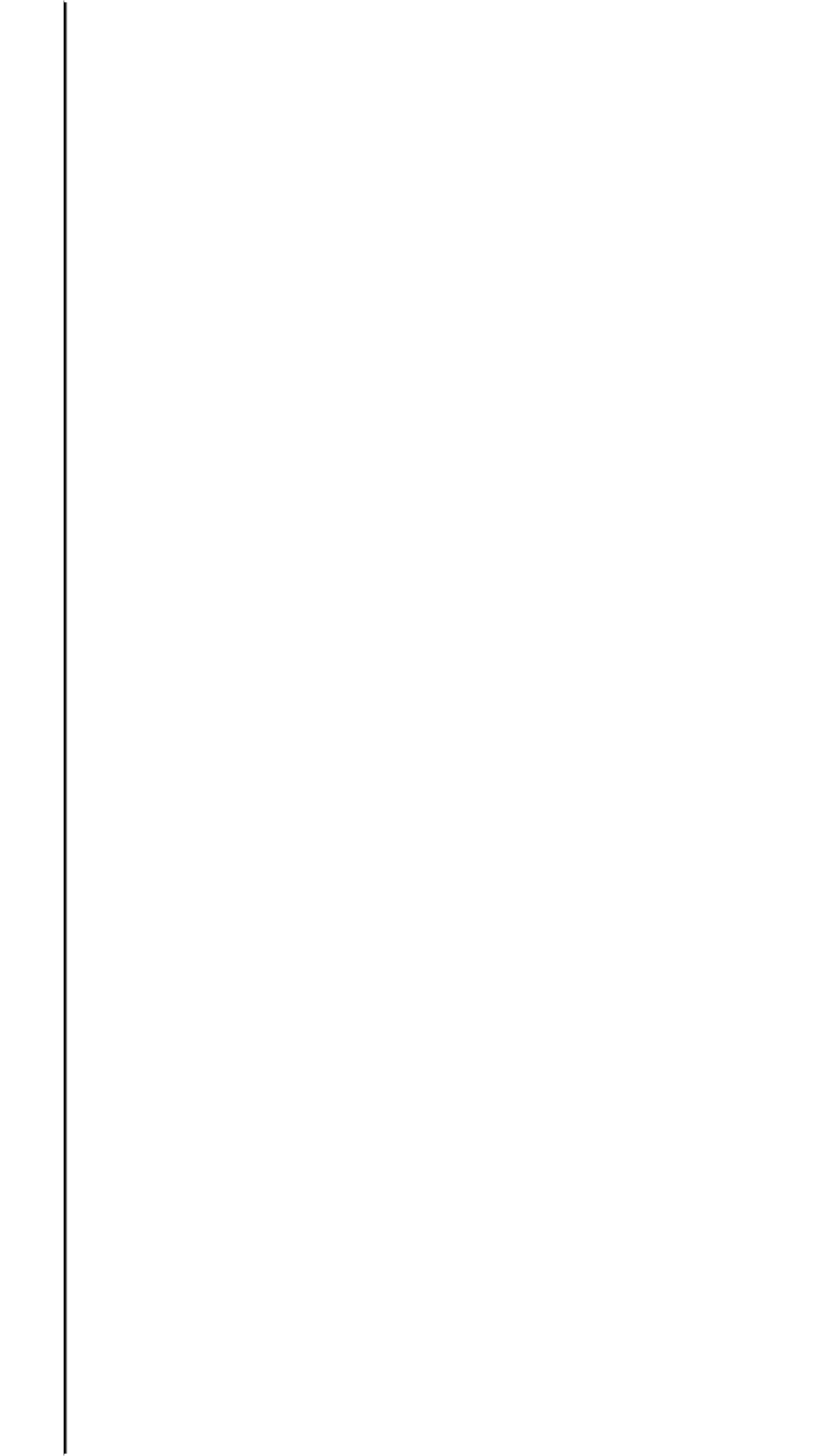
MOHAMMAD TAWRIT

SEPTEMBER, 1992



#85052#

DEPARTMENT OF ELECTRICAL AND ELECTRONIC ENGINEERING
BANGLADESH UNIVERSITY OF ENGINEERING AND TECHNOLOGY
DHAKA, BANGLADESH.

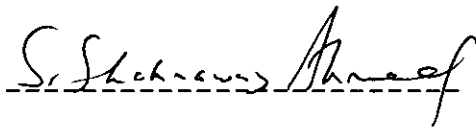


623.1913
1992
TAW

CERTIFICATE

This is to certify that this work was done by me and it has not been submitted elsewhere for the award of any degree or diploma.

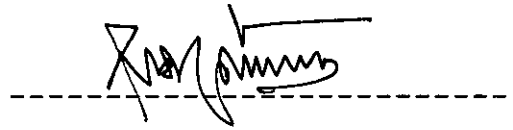
Countersigned



(Dr. S. Shahnawaz Ahmed)

Supervisor

Signature of the Candidate



(Mohammad Tawrit)

Accepted as satisfactory in partial fulfilment of the requirements for the degree of Master of Science in Engineering (Electrical and Electronic).

Board of Examiners:

(i)

S. Shahnawaz Ahmed 5/9/1992
(Dr. S. Shahnawaz Ahmed)

Chairman
(Supervisor)

Assistant Professor
Department of Electrical and
Electronic Engineering
BUET.

(ii)

Saiful Islam 5/9/92
(Dr. Saiful Islam)

Member

Professor and Head
Department of Electrical and
Electronic Engineering
BUET.

(iii)

Rahman 5/9/92
(Dr. Syed Fazl-i Rahman)

Member

Professor
Department of Electrical and
Electronic Engineering
BUET.

(iv)

Taifur Ahmed Chowdhury
(Dr. Taifur Ahmed Chowdhury)

Member

Associate Professor
Department of Electrical and
Electronic Engineering
BUET.

(v)

Md. Sekendar Ali 5/9/92
(Dr. Md. Sekendar Ali)
Director
Bangladesh Institute of Technology, Dhaka
Gazipur.

Member
(External)

ACKNOWLEDGEMENTS

It is a matter of great pleasure on the part of the author to acknowledge his profound gratitude to his Supervisor, Dr.S.Shahnawaz Ahmed, for his support, advice, valuable guidance, assistance and his constant encouragement throughout the progress of this research work.

The author also acknowledges his deep sense of gratitude to Professor Saiful Islam, Head of the Department, Professor Syed Fazl-i Rahman and Dr. Taifur Ahmed Chowdhury of Electrical and Electronic Engineering Department, BUET for showing interest and providing support and encouragement in this work.

The author also wishes to express his sincere thanks to the engineers (specially Mr. Wasim Farooque, Assistant Engineer, System Planning Directorate) of Bangladesh Power Development Board for providing him with the relevant data and other information on the national grid system.

ABSTRACT

In a particular bulk power transmission system the amount of power transfer can be increased by converting the widely used three phase double circuit lines into six phase single circuit lines instead of upgrading the transmission voltage. In this conversion process the existing conductors, towers and corridors of three phase lines can be used.

In this work, an extensive investigation has been made to determine the steady state power transferability, safety margin in line configuration, fault level and transient stability of three and six phase transmission lines through simplified, realistic and unified approaches. A specific line of Bangladesh Power Development Board grid system was studied in 132 KV six phase single circuit mode and the results were compared with those obtained from studies made also for 132 KV and 230 KV three phase double circuit modes.

The fault analysis and the transient stability study have been done for practical faults using new techniques without involving the symmetrical component method and its complexities.

A comprehensive analysis of the fault and stability studies together with numerical results has been presented in details.

TABLE OF CONTENTS

	<u>Page</u>
CHAPTER 1 INTRODUCTION	1
1.1 General Considerations	2
1.2 Review of Previous Works	2
1.3 Purpose of the Present Investigation	5
1.4 Organisation of the Thesis	6
CHAPTER 2 CHARACTERISTICS AND MODELLING OF THREE AND SIX PHASE LINES	7
2.1 Introduction	8
2.2 Characteristics of Three Phase Lines in BPDB System	8
2.3 Characteristics of A Six Phase Line	8
2.3.1 Phase Configuration for A Six Phase Line	10
2.3.2 Comparison of Safety Factors	12
2.4 Power Transferability	14
2.4.1 Calculation of Line Reactance	15
2.4.2 Comparison of Practical Power Transfer Limits	16
2.5 Modelling of the Three Phase Network and the Line under Study in 132 KV Three Phase Mode	18
2.5.1 Representation of the Line in 230 KV Three Phase Mode	20
2.5.2 Representation of the Line in 132 KV Six Phase Mode	21

	<u>Page</u>
2.6 Conclusions	22
CHAPTER 3 FAULT ANALYSIS	25
3.1 Introduction	26
3.2 Specification of Faults	26
3.3 Location of Faults	27
3.4 Application of Loop Current Method	27
3.4.1 Phase to Ground (L-G) Fault in 132 KV Three Phase Mode	28
3.4.2 Two-phase (L-L) Fault in 230 KV Three Phase Mode	29
3.4.3 Three-phase to Ground (L-L-L-G) Fault in 132 KV six Phase Mode	31
3.5 Results on Fault Levels	33
3.6 Conclusions	35
CHAPTER 4 TRANSIENT STABILITY ANALYSIS	36
4.1 Introduction	37
4.2 Determination of Critical Clearing Angle	37
4.3 Determination of Prefault Limit	39
4.4 Calculation of During-Fault Limit	39
4.4.1 Calculation of Power Transferred through the Phases of L-L Fault	40

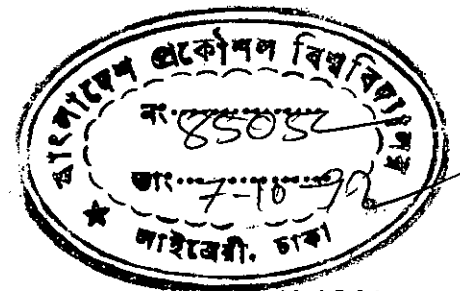
	<u>Page</u>
4.4.2 Calculation of Power Transferred through the Phases of L-L-L fault in Six Phase Mode	43
4.5 Determination of Postfault Limit	46
4.6 Results on Critical Clearing Angles	46
4.7 Conclusions	48
 CHAPTER 5 CONCLUSIONS	 49
5.1 Conclusions	50
5.2 Suggestions for Future Research	52
 REFERENCES	 54
APPENDIX A DERIVATION OF THE EXPRESSION OF STEADY STATE POWER TRANSFERABILITY	 A-1
APPENDIX B DERIVATION OF THE EXPRESSION FOR LINE INDUCTANCE	B-1
APPENDIX C DERIVATION OF THE EXPRESSION FOR CRITICAL CLEARING ANGLE	 C-1

LIST OF SYMBOLS AND ABBREVIATIONS

V_L	Voltage between two adjacent conductors
V_P	Phase to neutral voltage
D_G	Ground clearance
D_V	Vertical spacing
D_H	Horizontal spacing
S_G	Safety index regarding ground clearance
S_H	Safety index regarding horizontal clearance
S_V	Safety index regarding vertical clearance
P_{max}	Maximum limit of steady state power
V_s	Specified phase to neutral voltage magnitude at the sending end
V_R	Specified phase to neutral voltage magnitude at the receiving end
X	Total series reactance of the line per phase
P_{therm}	Practical limit of power (MW) transferable per phase
I_{therm}	The current carrying capacity of each of the conductors
E_{chg}	The Thevenin's emf at Ghorasal 132 KV bus
E_{chi}	The Thevenin's emf at Ishurdi 132 KV bus
X_{chg}	The Thevenin's reactance at Ghorasal 132 KV bus

X_{th1}	The Thevenin's reactance at Ishurdi 132 KV bus
δ	Swing angle
δ_{cr}	Critical clearing angle
P_m	Constant mechanical power delivered from the prime mover of the machine at the sending end of the line
P_{max}	Maximum electrical power that can be transferred from sending end to receiving end of the line in prefault condition
δ_0	Initial angle of swing at which a power equal to P_m was being supplied before fault from the sending end to the receiving end
r_1	The ratio of the maximum power transferable during fault to that before fault
r_2	The ratio of the maximum power transferable after clearing fault to that before fault
I.S.	Inherent stability
BPDB	Bangladesh Power Development Board
L-G	Single Line to Ground
L-L	Line to Line
L-L-G	Double Line to Ground
L-L-L	Three Phase
L-L-L-G	Three Phase to Ground

CHAPTER 1
INTRODUCTION



1.1 General Considerations

In view of growing demand for electrical energy, the possibility of increased power transfer by converting some of the existing double circuit lines of a three phase grid system into six phase single circuit lines has attracted the attention of contemporary researches. The main motivations behind this is the optimum utilization of existing rights-of-way instead of acquiring another corridor for a new line at an ever-increasing cost. The other alternative consisting in upgrading of the transmission line voltage, requires the replacement of the existing towers and lines and a wider corridor too. So it appears to be more costly than the six phase conversion scheme.

Since 1972, research effort has been put on the concepts, feasibilities, fault and stability analyses of six phase transmission system. A detailed list of it has been provided in the significant and representative works^{1-e}.

1.2 Review of Previous Works

Bhatt et al¹ proposed the use of a single set of six phase symmetrical components to analyze the four types of faults on a six phase line viz: single phase to ground fault, six-phase fault, three-phase to ground fault and five-phase to ground fault. The authors¹ themselves doubted whether the last three types of fault which did not involve vertically adjacent conductors, would ever occur. However, only the theory was developed without showing any numerical example.

Due to an apparent difficulty in extending the method¹ of six-phase symmetrical components to analyze all types of faults on a six-phase line, Venkata et al² proposed the use of the phase coordinate method. This method was adopted to analyze 23 fault combinations ranging from 'single-phase to ground fault' to 'six-phase fault' involving either adjacent or unadjacent conductors and ground or no ground, though most of them have little probability to occur in practice. To quantify the investigation, the authors² considered for six-phase conversion a specific line namely the Springdale-McClamont 138 KV three phase double circuit line in the Allegheny power system. However, the three-phase/six-phase transformer needed at either end of the line was not modelled at all rather its impedance was neglected resulting in a departure from a realistic analysis. Moreover, it was not clearly explained why the line impedance was considered the same for the three phase double circuit mode and the six-phase single circuit mode. Apart from that, the way the three phase source impedance at either end was correlated with the six phase line impedance, was not clear.

Tiwari et al³ carried out a single phase load flow analysis on a hypothetical 6-bus and 8-lines test system converting certain existing double circuit three phase lines into six phase single circuits with an over-emphasis on the modelling of six phase lines and three phase/six phase interfacing transformers. However, the models proposed for these elements appear to be based on difficult-to-follow derivations.

Chandrasekaran⁴ investigated into the transient stability aspect

of a six phase transmission line. A hypothetical test system consisting of a three phase generator connected to an infinite bus through a 138 KV three phase double circuit line, was considered. The line when considered in six phase mode was modelled as two three phase groups. The three phase to six phase transformer was considered as a three winding transformer plus a difficult-to-realize "ideal" 180° phase shifting transformer in series with the tertiary winding. In order to apply the three phase symmetrical component method it was assumed that the faults on the line occurred on only one of the three phase groups although the conductors belonging to the same phase group were not physically adjacent to each other. Consequently the faults investigated were only of theoretical interest.

Bhat et al⁵ presented the theory for analyzing a simultaneous ground and phase fault on the terminals of an unloaded six phase generator. However the concepts of the six phase generator and the type of the fault analyzed, both seem to be less familiar to the utility engineers. From practical as well as economic considerations it is accepted^{3,4} that six phase lines will always be integrated in an otherwise three phase system in which the generator remains essentially a three phase one.

Badawy et al⁶ proposed the theory of two sets of three phase symmetrical components in analyzing 23 fault combinations for a six phase line. The authors⁶ considered only the transmission line and excluded the three phase/six phase transformer in the proposed theory. Moreover, it was not clear why any numerical example was not reported.

1.3 Purpose of the Present Investigation

It appears that the treatments of the six phase transmission line in the previous publications¹⁻⁹ suffer from one or more of the drawbacks, mainly lack of simplicity in modelling, absence of in-depth analysis, inability to consider the phase conversion transformer, consideration of impractical faults, analysis of only one aspect and no quantitative comparison with 132 KV and 230 KV three phase modes.

The main areas in which the present research work contributes are as follows:

- 1) The effects of converting a three phase line into a six phase one in a practical grid system have been investigated through simplified as well as realistic modelling of the six phase line, the three phase/six phase transformer and the three phase network in which the line is embedded.
- 2) The justifications from practical stand point have been presented as regards to the choice of the types of fault for analysis.
- 3) The resulting network models during fault conditions have been analyzed using the loop current method for determining fault currents.
- 4) The equal area criterion method for transient stability analysis has been extended for all the practical faults through a new technique.
- 5) Same approach has been used for all the analyses in three phase and six phase modes of the line.
- 6) A specific line of Bangladesh Power Development Board (BPDB) grid

network has been chosen as an example and studied in three modes, namely 132 KV three phase double circuit, 230 KV three phase double circuit and 132 KV six phase single circuit mode. A number of important aspects such as safety factor, steady-state power transferability, fault level and transient stability limit in the three modes have been analyzed and compared comprehensively.

1.4 Organization of the Thesis

The presentation of the material studied in the present research project is organised as follows.

The concepts, configuration and model of a six phase line and also a comparison of its safety margin and power transferability with those of a three phase line have been provided in the Chapter 2.

The way the fault analysis was done and also a comparison of the fault levels, for practical faults in three and six phase modes have been presented in the Chapter 3.

The way the transient stability analysis was done for the three phase and six phase modes has been provided in the Chapter 4. Also a comparison of critical clearing angles for various faults in those modes has been shown.

Chapter 5 contains a summary of the main results obtained in the present research work and suggests some areas for future research.

The appendices include the mathematical derivations.

CHAPTER 2
CHARACTERISTICS AND MODELLING OF
THREE AND SIX PHASE LINES

2.1 Introduction

The system considered by the present research for study is Bangladesh Power Development Board (BPDB) transmission network. This is a three phase system basically at a grid voltage of 132 KV with the exceptions of a few lines which operate at 230 KV.

The line considered as an example for six phase conversion by the present work is 178 kilometer long three phase double circuit between Ghorasal and Ishurdi buses of the BPDB system.

2.2 Characteristics of Three Phase Lines in BPDB System

The typical characteristics for three phase double circuit lines at 132 KV and 230 KV have been shown in Table 2.1.

2.3 Characteristics of Six Phase Line

The conversion process of a 132 KV three phase double circuit line into a 132 KV six phase single circuit one requires a phase conversion transformer at its either end and does not involve any change in the 132 KV tower and the line itself. Therefore, in both 132 KV three phase double circuit and six phase single circuit modes of the line studied by this work, the tower height, ground clearance, conductor dimensions, thermal limit and the inter-conductor spacings, are the same as those for a typical 132 KV line mentioned in Table 2.1. However the phase configuration in the two modes are not the same.

Table 2.1: Typical characteristics of 3- ϕ double circuit lines in BPDB grid system.

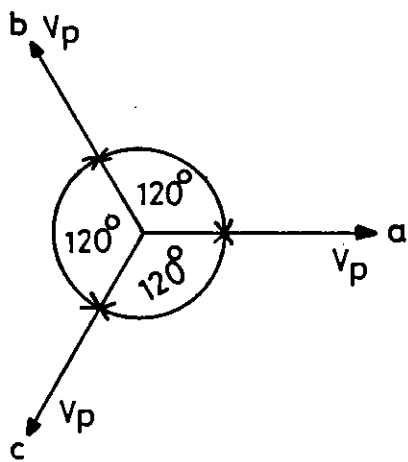
Voltage Level (KV)	Transmission tower height (metres)	Ground clearance D_g (metres)	Phase Configuration and inter-conductor spacing (distance in metres)	Conductor specifications (One conductor/cct./phase)	Thermal limit for loadability (MVA/cct.)
132	30	7	$aO-8.0-Oa$ \downarrow 4.2 \downarrow $bO-8.0-Ob$ \downarrow 4.2 \downarrow $cO-8.0-Oc$	Aluminium area: 477,000 Cmil ACSR, Hawk. Outside diameter: 21.7 mm GMR (D_g): 8.81mm	156
230	38	8	$aO-10.5-Oa$ \downarrow 6.0 \downarrow $bO-10.5-Ob$ \downarrow 6.0 \downarrow $cO-10.5-Oc$	Aluminium area 795,000 Cmil, ACSR, Mallard. Outside diameter: 28.8 mm GMR(D_g): 11.25 mm	315

Legend:

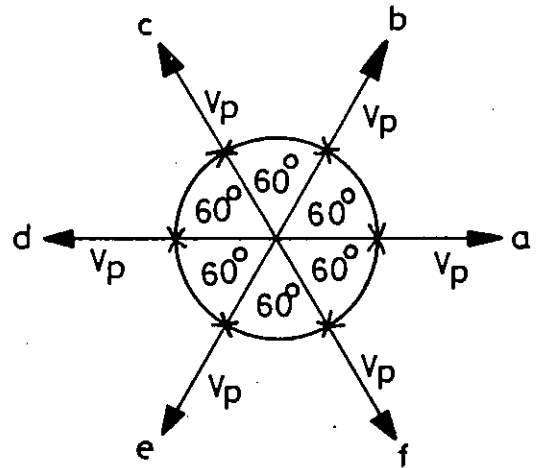
- cmil : Circular mil
- mm : milli-metre
- ACSR : Aluminium Conductors Steel Reinforced
- GMR : Geometric mean radius or self geometric mean diameter denoted by D_g
- a,b,c: notations for the three phases.
- D_g : denotes the distance between the ground and the lowest sag point of the line.

2.3.1 Phase Configuration for Six Phase Line:

While a set of three phase balanced voltages is shown as in Figure 2.1(a), the six phase voltages can be represented according to Figure 2.1(b).



(a)



(b)

Figure 2.1: Phasor representations of phase to neutral voltages for (a) a three phase double circuit and (b) a six phase single circuit.

It should be noted that the magnitude of the phase to neutral voltage V_P in Figure 2.1(a) is $132/\sqrt{3}$ KV and $230/\sqrt{3}$ KV respectively for a 132 KV three phase line and a 230 KV three phase line.

On the other hand the phase to neutral voltage V_P in Figure 2.1(b) is 132 KV for a 132 KV six phase line. Also the voltage between adjacent conductors V_L is 132 KV as evident^a from the following equation.

$$V_L = 2V_P \sin(180^\circ/n) \quad (2.1)$$

where n is the number of phases.

Equation (2.1) when applied to a three phase system confirms that the voltage between any two phases, V_L is 132 KV and 230 KV respectively for the 132 KV and 230 KV system.

In order to retain 132 KV between physically adjacent conductors of the six phase single circuit line, created by conversion of the 132 KV three phase double circuit, the phase configuration can be represented as in Figure 2.2 based on Figure 2.1(b).

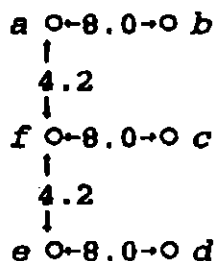


Figure 2.2: Phase configuration for the six phase single circuit line. The spacings are in meters.

It is worth-noting that the symbols used to label the conductors in Figure 2.2 are the same as corresponding phase notations. The voltages between the vertically adjacent conductors is 132 KV. The inter conductor spacings are the same as those for a typical 132 KV line of the BPDB system.

2.3.2 Comparison of Safety Factors

In order to assess the safety margins in converting a 132 KV double circuit configuration into a 132 KV six phase single circuit line, three indices have been defined as in equations (2.2) to (2.4).

$$S_G = D_G / V_{LN} \quad (2.2)$$

$$S_V = D_V / V_{VA} \quad (2.3)$$

$$S_H = D_H / V_{HA} \quad (2.4)$$

The significance and quantitative values of the indices and parameters in equations (2.2) to (2.4) have been provided in Table 2.2 for the line under consideration in both the modes and also compared with those obtainable in upgrading and replacing the line for 230 KV three phase double circuit mode.

It should be noted that the phase configurations and inter-conductor spacings used for the calculations in Table 2.2 are those shown in Table 2.1 and Figure 2.2.

In Table 2.2 two values of S_H have been shown for the six phase mode; these are 0.060 and 0.030 corresponding to $V_{HA}=132KV$ and 264 KV respectively.

Table 2.2: Comparison of safety factors for the line under consideration

Mode	Phase to neutral voltage (KV) VLN	Voltage between Conductors (KV)		Distances in metres			Safety indices (metres/KV)		
		Vertically adjacent VVA	Horizontally adjacent VHA	Ground clearance Dg	Vertical spacing Dv	Horizontal spacing Dh	Sg	Sv	Sh
132KV three phase double circuit	76.2	132	0	7	4.2	8.0	.092	.032	-
230KV three phase double circuit	132.8	230	0	8	6.0	10.5	.060	.026	-
132 KV six phase single circuit	132.0	132	132 between a and b 132 between e and d 264 between f and c	7	4.2	8.0	.053	.032	.060 and .030

The safety margin regarding ground clearance i.e. S_g apparently decreases in 230 KV three phase and 132 KV six phase modes relative to that in the 132 KV three phase mode. However based on two important points the safety margin obtained for six phase line can be considered acceptable.

i) Usually the transmission lines are designed conservatively such that the actually needed factor of safety is less than that shown as the typical value. As a result conversion of an already designed 132 KV 3- ϕ line into a 6- ϕ one will have practically insignificant effect on safety margin.

ii) The values of S_g obtained for 230 KV 3- ϕ and 132 KV 6- ϕ modes are close to each other. As the phase to neutral voltages for the two modes are almost the same and 230 KV three phase lines with the obtained safety factors are already in operation at some places of the BPDB system, S_g for 6- ϕ mode as found is also acceptable.

The safety index S_H regarding horizontal spacing of the line conductors in six phase mode is also acceptable when compared with that for vertical spacing i.e. S_v which is same as that for 132 KV 3- ϕ mode.

2.4 Power Transferability:

The maximum limit of the steady-state power, P_{max} , transferable to the receiving end of a transmission line, is assessed on per phase basis using the equation (2.5) whose derivation has been shown in Appendix A.

$$P_{\max} = (V_S * V_R)/X \quad (2.5)$$

where

V_S = specified phase to neutral voltage magnitude at the sending end

V_R = specified phase to neutral voltage magnitude at the receiving end

X = total series reactance of the line per phase

2.4.1 Calculation of Line Reactance

In reactance calculation often an assumption⁹ of complete transposition is made although the line is not transposed in practice to reduce possibility of fault occurrence. However, this assumption simplifies the calculations and provides a practical value for the reactance with an insignificant difference from the actual one.

In the present work the method⁹ of finding the average inductance of one conductor in a group of stranded conductors, has been used in both three phase and six phase modes of the line under study as shown in Appendix B. This method inherently takes into account the effect of mutual coupling which exists between the conductors belonging to the same as well as different phases.

For the three phase double circuit line the inductance per phase consisting of two conductors, was taken as half of the value of the average inductance obtained for a single conductor.

The values of the per phase reactance of the line under consideration has been provided for 132 KV and 230 KV three phase and 132 KV six phase modes in Table 2.3.

2.4.2 Comparison of Practical Power Transfer Limits

While equation (2.5) provides a theoretical limit of power transferability there is a constraint to it. This is mainly the thermal loadability limit which depends upon the current carrying capacity of the conductors used in the line. Consequently the practical limit becomes less than the theoretical one.

Table 2.3 provides a comparison of both theoretical and practical limits of power transferable through the line under study in its three modes.

Table 2.3: Comparison of Power transferability

Mode	Reactance at 50 Hz (Ohms/Phase)	Maximum Limit of Power Transferability in MW			
		Theoretical		Practical	
		Per phase	Total	Per phase	Total
132 KV 3 phase double circuit	44.29	131.13	393.39	104	312
230 KV 3 phase double circuit	45.22	389.93	1169.79	210	630
132 KV 6 phase single circuit	88.06	197.86	1187.16	90.07	540.42

In Table 2.3 the theoretical limit per phase has been calculated by equation (2.5) taking the voltage magnitude at both sending and

receiving ends as equal to the system's nominal phase to neutral voltage.

For the three-phase modes the practical limit per phase reported in Table 2.3 has been obtained from the corresponding data on thermal limit (MVA/circuit) shown in Table 2.2. A unity power factor was assumed for the maximum limit.

For the 132 KV six phase mode the per phase practical limit has been calculated using equation (2.6).

$$P_{\text{therm}} = V_{\text{LN}} * I_{\text{therm}} \quad (2.6)$$

where

P_{therm} = Practical (thermal) limit of power (MW)
transferable per phase.

V_{LN} = Phase to neutral voltage equal to 132 KV for the
six phase mode.

I_{therm} = the current carrying capacity of each of the
conductors in the 132 KV three phase mode, because
the same conductors will also be used in 132 KV six
phase mode.

The value of I_{therm} was obtained using equation (2.7).

$$\text{Thermal limit per circuit} = \sqrt{3} V_L I_{\text{therm}} \quad (2.7)$$

In equation (2.7) the thermal limit per circuit of the 132 KV 3- ϕ double circuit line was 156 MVA as specified in Table 2.2 and the phase to phase voltage V_L was 132 KV.

A comparison of the figures in Table 2.3 shows that the theoretical limit of total power transferable in 230 KV 3- ϕ and 132 KV 6- ϕ modes are respectively 2.97 and 3.01 times that in the 132 KV

3- ϕ mode.

However, if thermal loadability constraint is considered then the practical limit for the 230 KV 3- ϕ mode and 132 KV 6- ϕ mode becomes respectively 2.01 and 1.73 times that in the 132 KV 3- ϕ mode. But it should be noted that while the same conductors have been considered to be used in both 132 KV 3- ϕ and 6- ϕ modes, bigger sized conductors with higher current carrying capacity were considered for the 230 KV 3- ϕ mode.

2.5 Modelling of the Three Phase Network and the Line under Study in 132 KV Three Phase Mode

The line under consideration together with the surrounding three phase network phase network has been modelled based on the Thevenin's equivalent circuit representation⁹ of a power system. Figure 2.3 shows the model on per phase basis for the line in the mode of 132 KV three phase double circuit with a Thevenin's source at either end which has been considered to be solidly grounded.

The significance of the parameters used in the model shown in Figure 2.3 are as follows:

E_{thg} = the Thevenin's emf at Ghorasal 132 KV bus.

X_{thg} = the Thevenin's reactance at Ghorasal 132 KV bus.

E_{thi} = the Thevenin's emf at Ishurdi 132 KV bus.

X_{thi} = the Thevenin's reactance at Ishurdi 132 KV bus.

X = Line reactance per phase equal to 44.29 ohms as shown in Table 2.3.

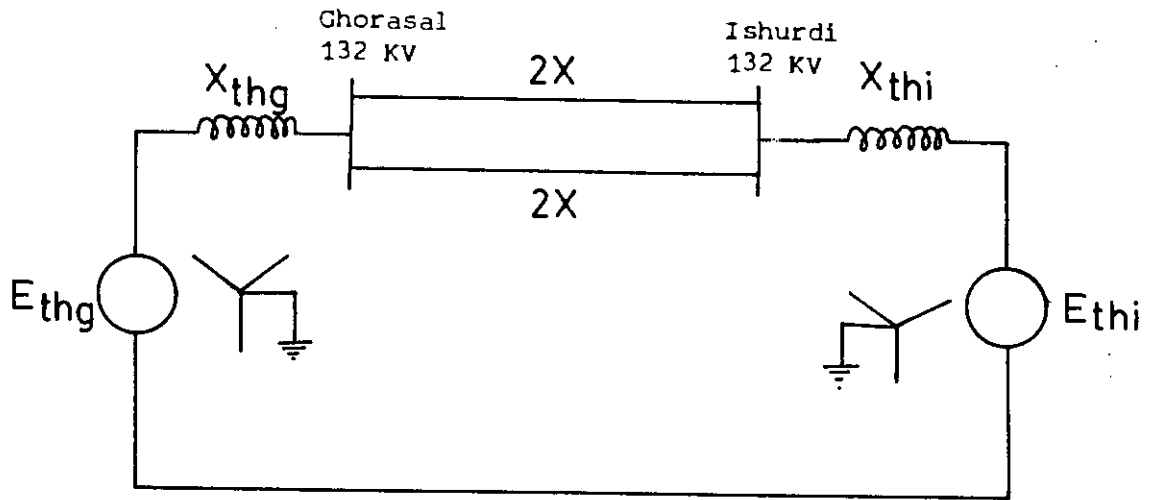


Figure 2.3: Model for the 3- ϕ double circuit line between 132 KV Ghorasal and Ishurdi buses of the BPDB network on per phase basis.

The values of the Thevenin's parameters have been desired from the fault data supplied by BPDB. The fault data were obtained through a fault analysis on the whole BPDB network excluding the line under study and considering a three-phase fault respectively at the Ghorasal 132 KV bus and then at the Ishurdi 132 KV bus. Table 2.4 shows the relevant fault data and also the Thevenin's parameters at those buses.

The values of X_{th} and E_{th} shown in Table 2.4 were obtained^a using equations (2.8) and (2.9) respectively.

$$X_{th} = (MVA_b / MVA_f) \quad (2.8)$$

$$E_{th} = I_f X_{th} \quad (2.9)$$

In equation (2.9) the values of I_f was considered in per unit.

Table 2.4: Data obtained from study on three-phase fault at Ghorasal and Ishurdi buses of the BPDB network.

Base Quantities	Bus	Fault current in Amps (I_f)	Fault MVA (MVA_f)	X_{th} in per unit (p.u.)	E_{th} in p.u. of base voltage to neutral
Base MVA (MVA_b)=100	Ghorasal 132 KV	12313	2815.13	0.036	1.01
Line-to-line base KV =132	Ishurdi 132 KV	6378	1458.21	0.069	1.0

2.5.1 Representation of the Line in 230 KV Three Phase Mode

The model of the line in 132 KV three phase mode shown in Figure 2.3 has been extended for that in the 230 KV 3- ϕ mode as in Figure 2.4 .

The values of the Thevenin's parameters shown in Figure 2.4 are the same as those shown in Table 2.4 . The line reactance per phase, X , is 45.22 ohms as shown in Table 2.3 . The two transformers in parallel at either end of the line are identical. Each of them is a bank of three single-phase transformers each rated 75 MVA, $(132/\sqrt{3})/(230/\sqrt{3})$ KV & 13% impedance. The transformer data was provided by BPDB.

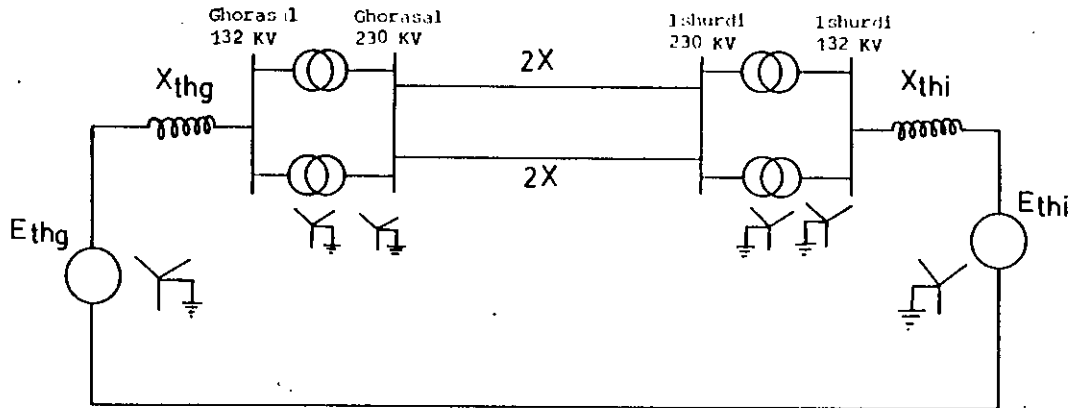


Figure 2.4: Model on for the Ghorasal-Ishurdi line in the 230 KV 3- ϕ double circuit mode on per phase basis.

2.5.2 Representation of the Line in 132 KV Six Phase Mode

In 132 KV six phase single circuit mode the line has been modelled as shown in Figure 2.5 .

The values of the Thevenin's parameters shown in Figure 2.5 are the same as those provided in Table 2.4 .

The line reactance of the six phase line is $X=88.06$ ohms/phase as given in Table 2.3.

Each of the three phase/six phase transformer at either end of the line has been proposed to be a bank of three single phase transformers each rated 75 MVA and $(132/\sqrt{3})/264$ KV. The high-tension winding of each single phase transformer is grounded at the centre

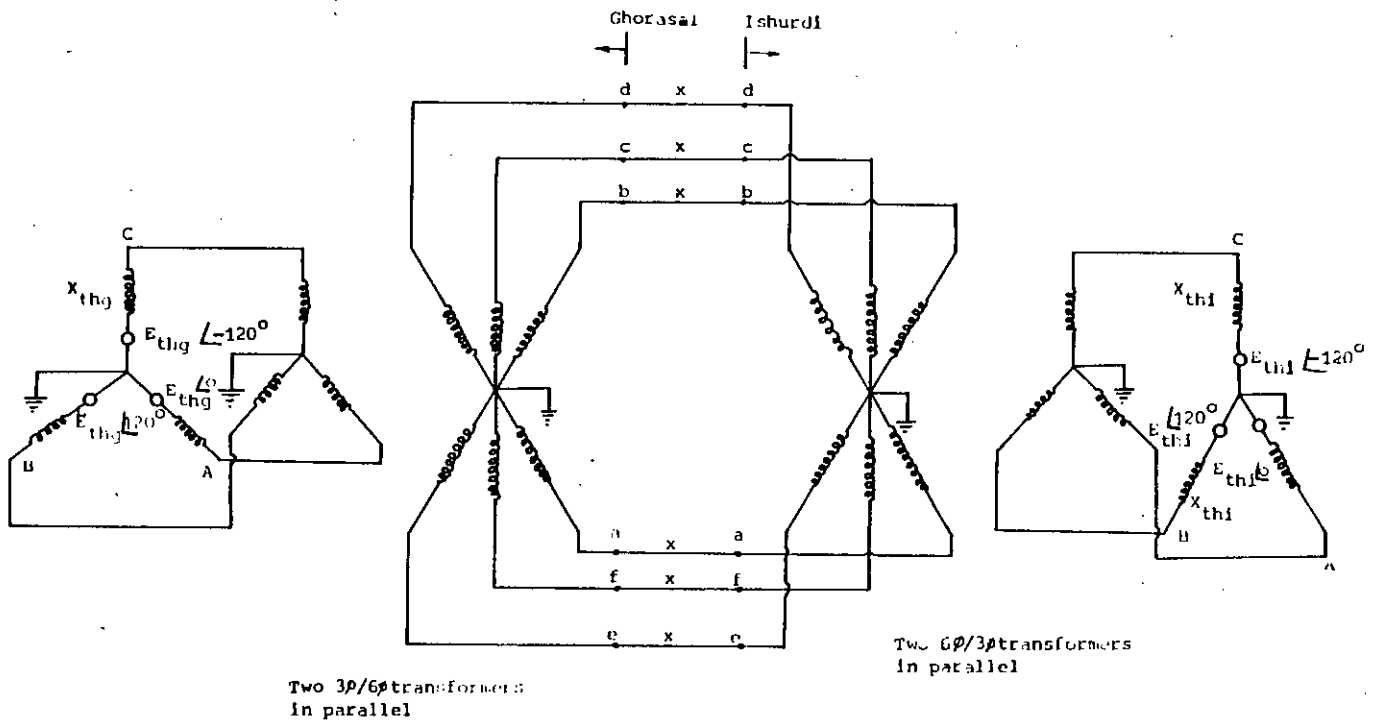


Figure 2.5: Model for the Ghorasal-Ishurdi line in six phase single circuit mode.

point so that 132 KV would appear between each terminal and the centre point. The equivalent reactance of the low-tension and each half of the high-tension winding has been considered as 13% based on the proposed rating. The centre points of high-tension windings of all the three single-phase transformers are connected together to the ground as shown in Figure 2.5 .

2.6 Conclusions

The three phase double circuit line between Ghorasal and Ishurdi of BPDB grid system was considered as an example for conversion into a six phase single circuit. The line would have same characteristics excepting phase configuration in the 132 KV 3- ϕ double circuit mode and the 132 KV 6- ϕ single circuit mode. A phase configuration has been proposed for the six phase line ensuring 132 KV between its vertically adjacent conductors. The effects of the six phase conversion with proposed phase configuration, upon the safety margin have been quantified and compared by defining three indices for both three and six phase modes in terms of the inter-conductor voltage, horizontal and vertical spacings and ground clearance. The per phase steady state power transferability and line reactance calculations have been done using the same method for both three and six phase lines.

The line under consideration and the three phase network in which it is embedded, have been modelled on the basis of Thevenin's equivalent circuit representation at two 132 KV buses, one at each of the line. The Thevenin's emfs and the corresponding series reactances

remained the same in the three models of the line corresponding to its three modes. However in the model for the 230 KV three phase mode, step up (132KV/230KV) and step down (230KV/132KV) transformers were added respectively after and before the 132 KV buses. Also the line has been considered to have been replaced by one with different geometric size and spacings appropriate for upgrading line voltage to 230 KV. In the model of 132 KV six phase mode, while the line remained the same as that for 132 KV three phase mode, phase conversion transformers (3- ϕ /6- ϕ and vice versa) were added respectively after and before the sending and receiving end three phase buses. Simple and practical models have been proposed for these transformers. The models derived in three modes of the line can be used for fault and transient stability analysis.

The configurational safety factors and power transferability (from thermal point of view) of the line in 132 KV six phase mode have been compared with those in 132 KV three phase mode and also with those obtainable in upgrading and replacing the line for 230 KV three phase double circuit. It has been observed that conversion of an existing 132 KV three phase double circuit line into a six phase single circuit one without changing the tower and line conductors is more favourable than upgrading and replacing the line for 230 KV with bigger sized conductors on a new tower.

CHAPTER 3
FAULT ANALYSIS

3.1 Introduction

The common faults on three phase transmission lines are single phase to ground, two-phase and three-phase faults. For the three phase double circuit line with the conductors arranged on the two lateral sides of the tower, the two-phase or three-phase faults involve the adjacent conductors on the same side. When this line would be converted into a six phase single circuit one, then also there are three conductors on each side. As a result the two-phase or three-phase fault on the six phase line will also involve only adjacent conductors. Based on this practical consideration, the types of faults chosen for analysis by the present work are those which involve one or more of the three conductors on the same side.

3.2 Specification of Faults

The selected faults have been shown in Table 3.1. It should be noted that the symbols used to specify types of faults for the three phase mode mean the conductors a,b,c of one side (circuit) only not both the sides (circuits).

In the three phase mode the L-L-L-G fault is the same as L-L-L fault since no current flows to the ground under this balanced fault condition. Also, in 3- ϕ mode the other combinations for L-L or L-L-G fault are insignificant because of 132 KV voltage between any pair of the three conductors. But for six phase mode there are two significant combinations for L-L and L-L-G faults because of 132 KV between a and f while $132 \times \sqrt{3}$ KV between a and e, on the basis of the phasor diagram shown in Figure 2.1(b).

Table 3.1: Types of faults selected for analysis

Mode	phase configuration	Types of faults				
		L-G	L-L	L-L-G	L-L-L	L-L-L-G
132 or 230 KV three phase double circuit	<p>a o o a</p> <p>b o o b</p> <p>c o o c</p>	a-G	a-b	a-b-G	a-b-c	-
132 KV six phase single circuit	<p>a o o b</p> <p>f o o c</p> <p>e o o d</p>	a-G	<p>i)a-e</p> <p>ii)a-f</p>	<p>i)a-e-G</p> <p>ii)a-f-G</p>	a-f-e	a-f-e-G

Legend:

L: phase conductor
G: ground

3.3 Location of Faults

In the present work the faults have been considered to occur at the sending end of the line i.e. close to the Ghorasal bus, in all the three modes so that a comparison can be made corresponding to the worst fault location.

3.4 Application of Loop Current Method

The way the method^a of loop current was applied for analyzing the selected faults (mentioned in Table 3.1) in the three modes of the line under study, has been illustrated and clarified through three

sample examples respectively in sections 3.4.1 to 3.4.3 . These examples have been presented respectively on analyzing a phase to ground (L-G) fault in 132 KV three phase mode, a two-phase i.e. phase to phase (L-L) fault in 230 KV three phase mode and a three-phase to ground (L-L-L-G) fault in 132 KV six phase mode.

It should be noted that for simplifying the fault analysis retaining the accuracy needed from practical point of view, the contributions towards the fault current from the unfaulted phases are considered⁹ as zero. Based on this consideration, the unfaulted conductors have been omitted in Figures 3.6 to 3.8 respectively in sections 3.4.1 to 3.4.3 .

3.4.1 Phase to Ground (L-G) Fault in 132 KV Three Phase Mode

Based on the model shown in Figure 2.3, the fault at the sending end between conductor a and the ground in one of the two parallel circuits of the 132 KV 3- ϕ line has been analyzed as in the Figure 3.1 .

In Figure 3.1 all the parameters have been shown in per unit values on the base of 100 MVA and 132 KV line to line. On this base, the line reactance, $2X=2(44.29)$ ohms/phase/circuit is 0.5084 per unit.

The equations for loop currents I_g and I_1 are as follows.

$$1.01 \angle 0 = (j0.036)I_g \quad (3.1)$$

$$-1.0 \angle 0 = (j0.069 + j0.2542) I_1 \quad (3.2)$$

The fault current I_f i.e. the current from phase a to ground is obtained in per unit from equations (3.3) after solving equations

(3.1) and (3.2) .

$$I_f = I_g - I_1 \tag{3.3}$$

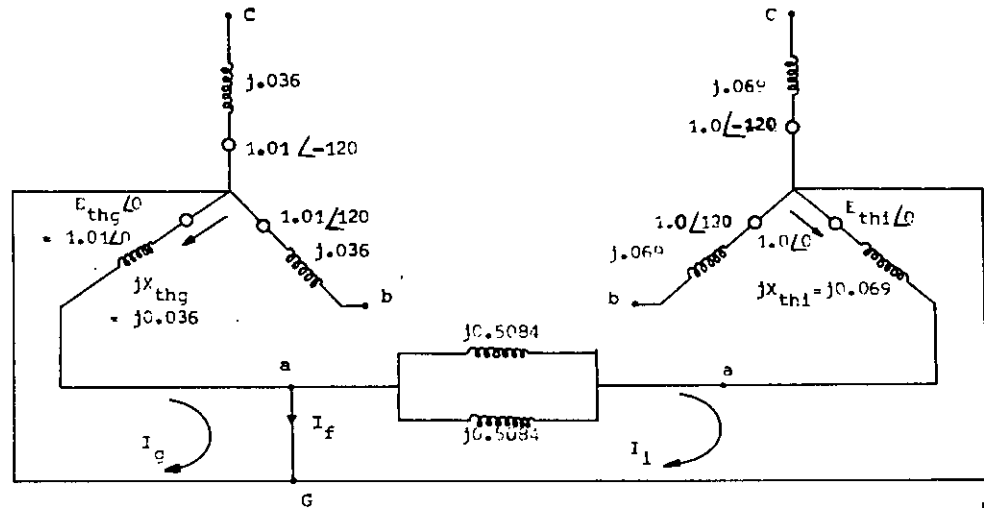


Figure 3.1: Analysis of a L-G fault on the 132 KV 3- ϕ line using loop current method.

3.4.2 Two-phase (L-L) Fault in 230 KV Three Phase Mode

Based on the model shown in Figure 2.4, the fault between the conductors a and b just near the Ghorasal bus in one of the double circuits of the 230 KV three phase line has been analyzed as in the Figure 3.2 .

In Figure 3.2 all the parameters have been shown in per unit with reference to the base of 132 KV line to line in the low-tension side while 230 KV line to line in the high-tension side and 100 MVA. On this base the line reactance, $2X=2(45.22)$ ohms/phase/circuit is

0.171 per unit. The reactance of two transformers in parallel at either end is 0.029 per unit on the same base.

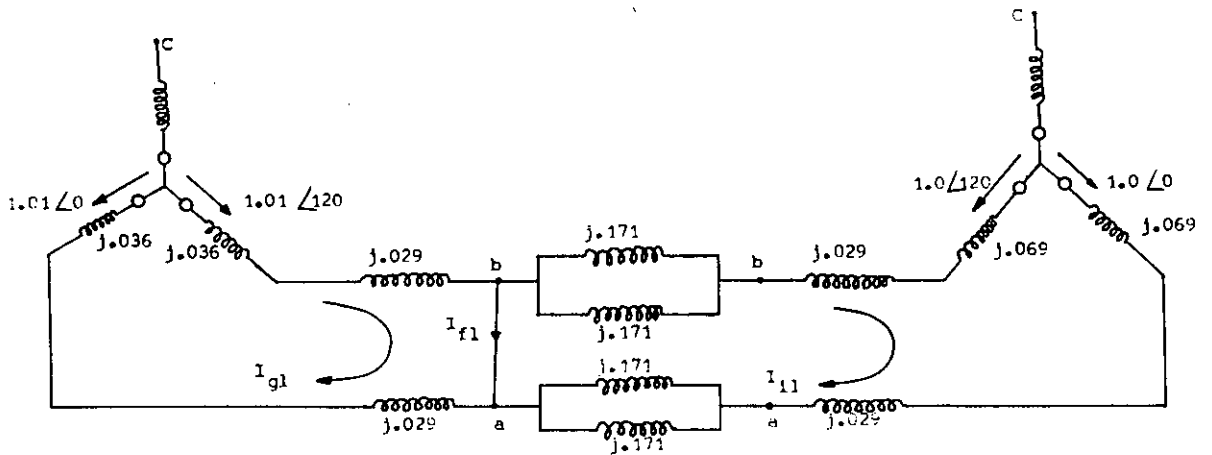


Figure 3.2: Analysis of a L-L fault on the 230 KV 3- ϕ line using loop current method.

The equations for loop currents I_{g1} and I_{l1} are as follows.

$$1.01 \angle 120 - 1.01 \angle 0 = 2(j0.036 + j0.029) I_{g1} \quad (3.4)$$

$$1.0 \angle 0 - 1.0 \angle 120 = 2(j0.0855 + j0.029 + j0.069) I_{l1} \quad (3.5)$$

The fault current I_{f1} i.e. the current from phase b to a is obtained in per unit from equation (3.6) after solving equations (3.4) and (3.5) .

$$I_{f1} = I_{g1} - I_{l1} \quad (3.6)$$

3.4.3 Three-phase to Ground (L-L-L-G) Fault in 132 KV six Phase Mode

Based on the model shown in Figure 2.5, the fault between the conductors a, f, e and the ground close to the Ghorasal bus of the 132 KV six phase single circuit line has been analyzed as in the Figure 3.3 .

It should be noted that the rated voltages between any pair of the phases a, c and e, on the six phase side or the high-tension side of the transformer shown in Figure 2.5, are $132 * \sqrt{3}$ KV based on the phasor diagram of Figure 2.1(b) . Similarly the voltages between other three phases b, d and f are $132 * \sqrt{3}$ KV. Therefore a choice of base equal to 100 MVA and 132 KV (line to line) in the three phase or low-tension side of the phase conversion transformer fixes the base as 100 MVA and $132 * \sqrt{3}$ KV (line to line) for each of the two groups - (i) a,c,e and (ii) b,d,f - on the six phase side.

On this base, the line to neutral Thevenin's emf at Ghorasal and Ishurdi ends remain the same (i.e. 1.01 p.u. and 1.0 p.u. respectively) when expressed in per unit and referred to the high tension side, as shown in Figure 3.3. In Figure 3.3 the phase angles of Thevenin's emfs have been shown as 0° , -60° , -120° respectively for the phases a, f and e based on Figure 2.1 (b).

It is also worth-mentioning that with the above-mentioned choice of base quantities, the Thevenin's reactance remain the same i.e. 0.036 p.u. and 0.068 p.u. respectively at Ghorasal and Ishurdi while the combined reactance of two phase conversion transformers in parallel at either end is 0.029 p.u. and the reactance of the each phase of the six phase line, $X=88.06$ ohms is 0.1885 p.u. as shown in

Figure 3.3 .

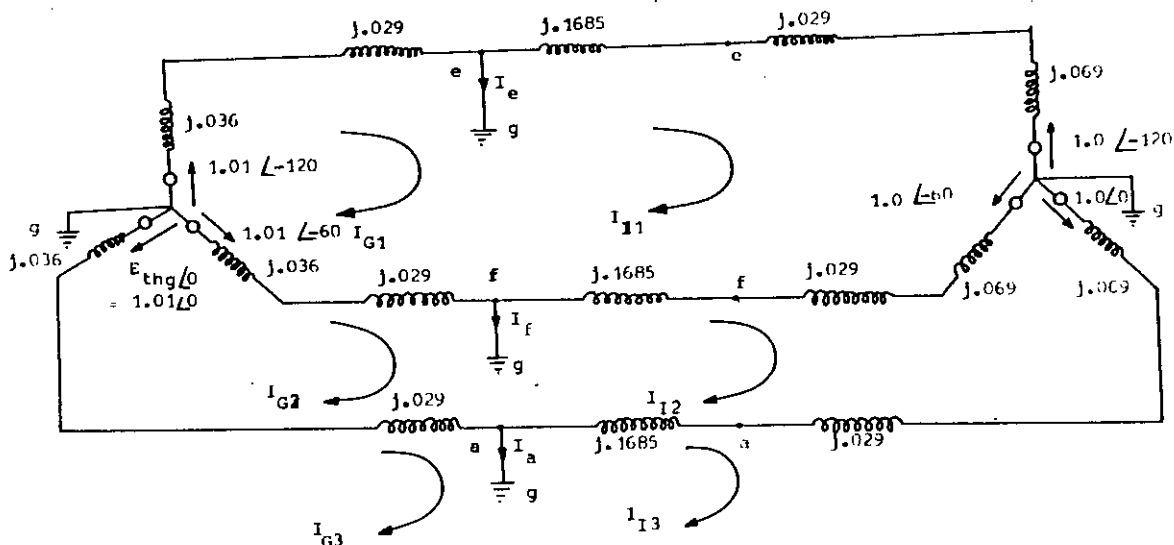


Figure 3.3: Analysis of a L-L-L-G fault on the 132 KV 6- ϕ line using loop current method.

The equations for the loop current I_{G1} , I_{G2} , I_{G3} , I_{11} , I_{12} and I_{13} are as follows.

$$1.01\angle-120 = j X_G I_{G1} \tag{3.7}$$

$$1.01\angle-60 = j X_G I_{G2} \tag{3.8}$$

$$1.01\angle 0 = j X_G I_{G3} \tag{3.9}$$

$$-1.01\angle-120 = j X_I I_{11} \tag{3.10}$$

$$-1.01\angle-60 = j X_I I_{12} \tag{3.11}$$

$$-1.01\angle 0 = j X_I I_{13} \tag{3.12}$$

The values of X_G and X_I are respectively as in equations (3.13) and (3.14)

$$X_G = 0.036 + 0.029 = 0.065 \tag{3.13}$$

$$X_I = 0.1685 + 0.029 + 0.069 = 0.2665 \quad (3.14)$$

After solving equations (3.7) to (3.14) the currents from phase e, f and a to the ground are obtained in per unit respectively from equations (3.15), (3.16) and (3.17).

$$I_e = I_{G1} - I_{I1} \quad (3.15)$$

$$I_f = I_{G2} - I_{I2} \quad (3.16)$$

$$I_a = I_{G3} - I_{I3} \quad (3.17)$$

3.5 Results on Fault Levels

The fault currents, determined through the application of the loop current method, for each of the selected fault types (specified in Table 3.1) have been shown in Table 3.2. Also the corresponding fault levels have been provided in the same Table.

In Table 3.2 the currents in per unit have been multiplied by respective base currents for conversion into Kilo-amperes. With the choice of base KV and MVA as mentioned in sections 3.4.1 to 3.4.3, the base currents in the line circuit are 437.38, 251.02 and 252.52 amperes respectively for 132 KV three phase, 230 KV three phase and 132 KV six phase modes.

It should be noted that the fault levels (MVA) for the faults involving phase(s) and ground, have been computed⁷ by summing together the product terms of system phase to neutral voltage (KV) and the current (Kilo-amps) from the faulted phases(s). This formula has also been applied for the L-L-L fault in three phase systems.

The fault level for two-phase i.e. L-L faults have been determined⁷ by multiplying together the fault current and the

Table 3.2: Fault levels in three modes of the line for fault at the sending end

Type of fault	phase	Currents from faulted phases							Fault level in MVA		
		132 KV three phase double cct.		230 KV three phase double cct.		132 KV six phase single cct.			132 KV three phase	230 KV three phase	132 KV six phase
		p.u.	kilo amps	p.u	kilo amps	phase	p.u.	kilo amps			
L-G	a	31.14 $\angle -90^\circ$	13.62	2 $\angle -90^\circ$	5.27	a	19.3 $\angle -90^\circ$	4.87	1038	700	643
L-L*	a	-26.97 $\angle 60^\circ$	11.78	-18.18 $\angle 60^\circ$	4.56	a	-16.7 $\angle 120^\circ$	4.22			965
	b	26.97 $\angle 60^\circ$	11.78	18.18 $\angle 60^\circ$	4.56	e	16.7 $\angle 120^\circ$	4.22	1555	1049	
						a	-9.6 $\angle 150^\circ$	2.42			
						f	9.6 $\angle 150^\circ$	2.42			319
L-L-G*	a	31.14 $\angle -90^\circ$	13.62	21 $\angle -90^\circ$	5.27	a	19.3 $\angle -90^\circ$	4.87			1286
	b	31.14 $\angle 30^\circ$	13.62	21 $\angle 30^\circ$	5.27	e	19.3 $\angle -210^\circ$	4.87	2076	1400	
						a	19.3 $\angle -90^\circ$	4.87			
						f	19.3 $\angle -150^\circ$	4.87			1286
L-L-L	a	31.14 $\angle -90^\circ$	13.62	21 $\angle -90^\circ$	5.27	a	17 $\angle -49^\circ$	4.29			
	b	31.14 $\angle 30^\circ$	13.62	21 $\angle 30^\circ$	5.27	f	6.4 $\angle -150^\circ$	1.62	3114	2100	
	c	31.14 $\angle -210^\circ$	13.62	21 $\angle -210^\circ$	5.27	e	17 $\angle 109^\circ$	4.29			1133
L-L-L-G	same as L-L-L					a	19.3 $\angle -90^\circ$	4.87			
						f	19.3 $\angle -150^\circ$	4.87	same as L-L-L		1929
						e	19.3 $\angle 150^\circ$	4.87			

Legend : L: Phase conductor G: ground
 * for six phase two combinations: a-e and a-f

prefault system voltage between those two phases.

The fault level for the L-L-L fault involving a-f-e phases in six phase mode has been obtained by adding the product $V_{ef}I_e$ with the product $V_{af}I_a$. The fault currents from phases e and a respectively, I_e and I_a are 4.29 Kilo-amps each as shown in Table 3.2. The prefault system voltage between phases e and f i.e. V_{ef} is 132 KV based on the phasor diagram of Figure 2.1(b). Similarly V_{af} is also 132 KV.

3.6 Conclusions

The fault analysis for practical faults, both balanced and unbalanced involving vertically adjacent conductors of the line, has been done in all the modes in a simple way applying the loop current method and without requiring the complexities of the symmetrical component method.

A comparison of the fault levels for the three modes shows that for the same type and location of a fault, the six phase lines fault level is the least one. The maximum fault-level occurs for the three-phase to ground(L-L-L-G) in both three phase and six phase modes. For this case, the fault level in the 132 KV six phase mode is respectively about 62% and 92% of that in the 132 KV three phase and 230 KV three phase modes.

CHAPTER 4
TRANSIENT STABILITY ANALYSIS

4.1 Introduction

In the present work the equal area criterion⁹ has been considered to find out the transient stability limit in terms of the critical clearing angle. Critical clearing angle is the highest permissible swing between two synchronous machines such that if at or before this value of swing, the fault occurring on the line connecting the two machines is cleared their synchronism can be restored.

4.2 Determination of Critical Clearing Angle

A generalized formula⁹ for the critical clearing angle is as in equation (4.1) whose derivation has been shown in Appendix C.

$$\delta_{cr} = \cos^{-1} \left[\frac{\frac{P_m}{P_{max}} (\delta_{max} - \delta_o) + r_2 \cos \delta_{max} - r_1 \cos \delta_o}{r_2 - r_1} \right] \quad (4.1)$$

where

δ_{cr} = Critical clearing angle in units of radian

P_m = Constant mechanical power delivered from the prime mover of the machine at the sending end of the line.

P_{max} = Maximum electrical power that can be transferred from sending end to receiving end of the line in pre-fault condition.

$$\delta_o = \sin^{-1}(P_m/P_{max}) \quad (4.2)$$

is initial angle of swing at which a power equal to P_m was being supplied before fault from the sending end to the receiving end.

$$\delta_{max} = \pi - \sin^{-1}(P_m/r_2 P_{max}) \quad (4.3)$$

is maximum limit of swing after clearing the fault at δ_{cr} such that the two machines remain in synchronism.

$$r_1 = P_{maxd}/P_{max} \quad (4.4)$$

is the ratio of the maximum power transferable during fault (P_{maxd}) to that before fault (P_{max}).

$$r_2 = P_{maxe}/P_{max} \quad (4.5)$$

is the ratio of the maximum power transferable after clearing fault (P_{maxe}) to that before fault (P_{max}).

Equation (4.1) requires determination of the pre-fault, the during-fault and the post-fault maximum limits of power transferability respectively denoted by P_{max} , P_{maxd} and P_{maxe} . A common basis for their determination is the consideration⁹ that the emfs of the sources, at two ends of the line, remain constant.

In the present work each of the above three limits has been determined for both the faulted and the unfaulted phases and then the total of individual phase limits was considered to compute the ratios r_1 and r_2 required by equation (4.1). This way of calculation has facilitated application of equation (4.1) for both balanced and unbalanced faults in a simple manner.

For the line under study the two Thevenin's sources respectively at the Ghorasal and Ishurdi end as shown in Figures 2.3 to 2.5, have been considered as two machines. Also it has been considered that various types of faults occurred on the line at the worst point i.e. very close to the sending end bus at Ghorasal, as mentioned in

section 3.3, and a power of $P_m = 1.0$ p.u. was being supplied through the line from Ghorasal to Ishurdi before occurrence of the faults. Based on these considerations, the critical clearing angles have been determined using equation (4.1) in the three modes of the line corresponding to each of the selected fault types mentioned in Table 3.1 .

4.3 Determination of Prefault Limit

The prefault limit P_{max} has been calculated for each phase using equation (4.6).

$$\text{Per phase } P_{max} = E_{thg} * E_{thi} / X_T \quad (4.6)$$

where

X_T = Total impedance (per unit) in each phase between two emf sources.

E_{thg}, E_{thi} = Same significance as mentioned in section 2.5 .

4.4 Calculation of During-Fault Limit

With the exception of few cases, the power transferable through the phases(s) having a fault very close to the sending end bus is zero. In such a situation the power transferability P_{maxd} has been calculated by applying equation (4.6) to each of the unfaulted phases and then adding the limits together. This simple method has been adopted for all the modes to make the comparison fair.

The above mentioned exceptions are the L-L fault in both three and six phase modes and the L-L-L fault in only the six phase mode. For these cases, some power is transferred also through the affected

phases despite fault at the sending end. This transferred power needs to be added to the total of all the limits obtained by applying equation (4.6) to each of the unfaulted phases.

4.4.1 Calculation of Power Transferred through the Phases of L-L Fault

For a L-L fault at a point P, close to the sending end bus, only the affected phases have been modelled as in Figure 4.1 .

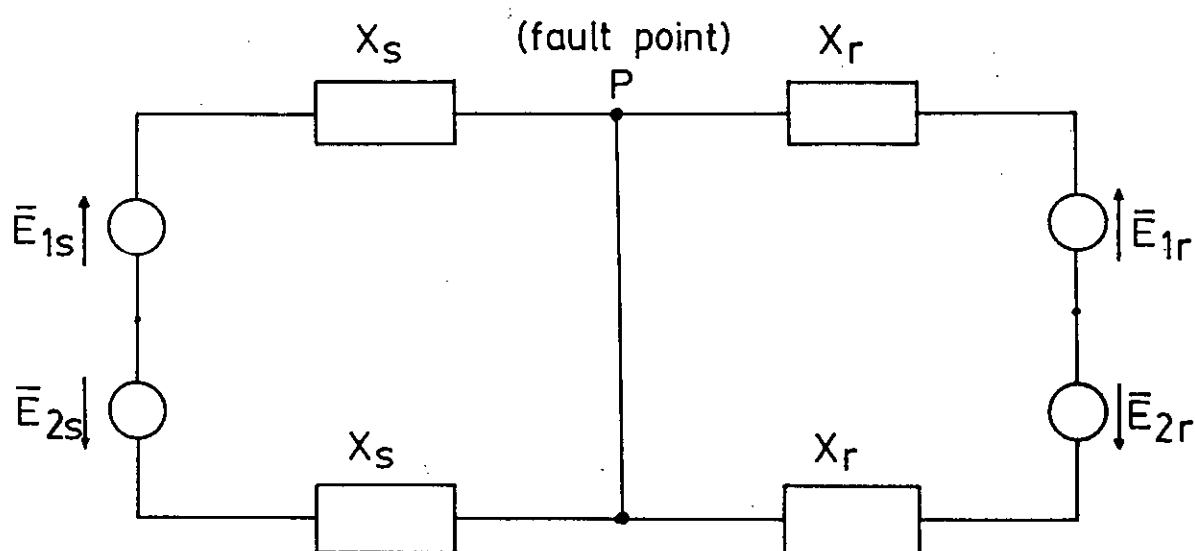


Figure 4.1: Modelling of a L-L fault

In Figure 4.1 \bar{E}_{1s} and \bar{E}_{1r} are respectively the phasor values of sending end and receiving end source emfs in phase-1 of the affected phases. Similar significance holds good for \bar{E}_{2s} and \bar{E}_{2r} in phase-2 . X_s is the total impedance in each phase between the

sending end source point and the fault point on the line. X_r is the total impedance in each phase between the fault point and the receiving end source point.

Each of the two e.m.f sources along with their respective reactance in series on either side of the fault point P, can be converted into a current source with a parallel conductance reciprocal of the corresponding reactance as shown in Figure 4.2 .

The two pairs of current sources together with their parallel conductances of Figure 4.2 have been reconverted respectively into two single e.m.f sources with two corresponding series reactances as in Figure 4.3 . Then the power transferability, P_f between two ends of the faulted phases have been computed by equation (4.7).

$$P_f = \frac{(\bar{E}_{1s} + \bar{E}_{2s}) * (\bar{E}_{1r} + \bar{E}_{2r})}{2(X_s + X_r)} \quad (4.7)$$

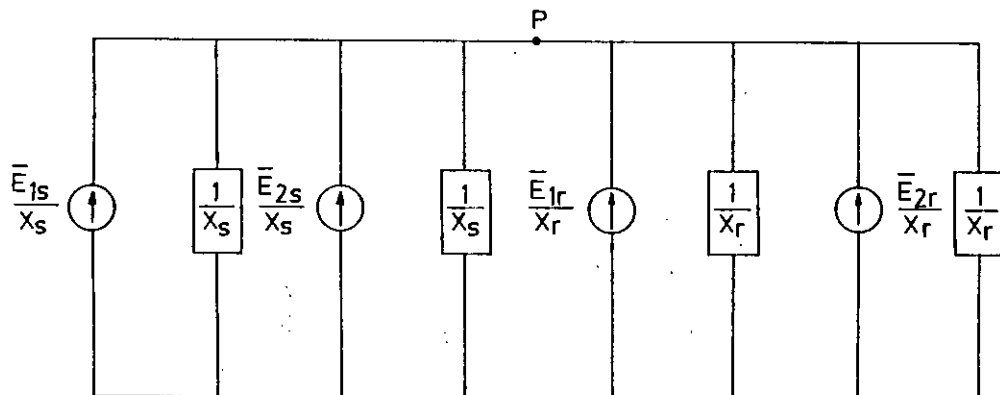


Figure 4.2: Conversion of e.m.f sources of Figure 4.1 into current sources

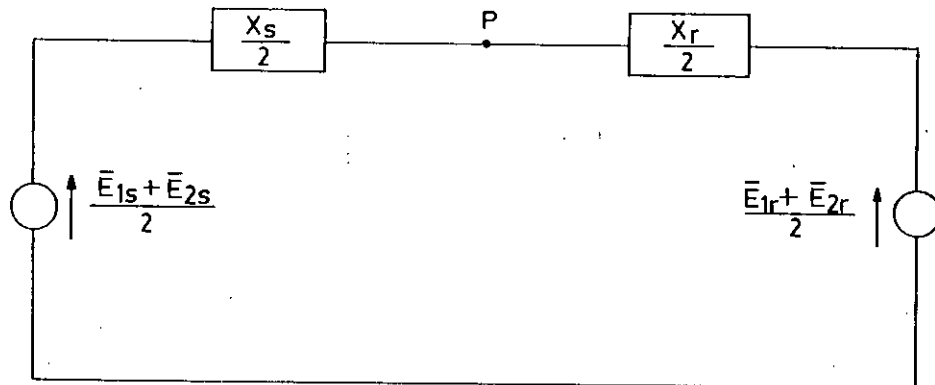


Figure 4.3: Simplification of model of Figure 4.2 by reconversion of current sources into e.m.f sources.

P_{maxd} for the L-L fault is then calculated by adding P_f to the total of the limits obtained from equation (4.6) applied to each of the unfaulted phases.

Table 4.1 shows the per unit values of the parameters \bar{E}_{1s} , \bar{E}_{2s} , \bar{E}_{1r} , \bar{E}_{2r} , X_s and X_r on respective bases in the three modes of the line studied by the present work. Figures 3.1 to 3.3 are also helpful in understanding the way these parameters have been determined.

It should be noted that due to consideration of fault at a point close to the sending end bus, reactances of both the circuit of the affected phases in three phase mode have been included in calculating X_r .

176

Table 4.1: Parameters (in p.u.) involved in computing the power transferable through the two phases affected by L-L fault at sending end.

Mode	132 KV 3- ϕ double cct.	230 KV 3- ϕ double cct.	132 KV 6- ϕ single cct.	
Phases considered	a-b	a-b	a-e	a-f
E_{1s}	1.0178	1.0178	1.0178	1.0178
E_{2s}	1.017(120+ δ)	1.017(120+ δ)	1.017(-120+ δ)	1.017(-60+ δ)
E_{1r}	1.070	1.070	1.070	1.070
E_{2r}	1.07120	1.07120	1.07-120	1.07-60
X_s	.0360	.0650	.0650	.0650
X_r	.3231	.1835	.2665	.2665

4.4.2 Calculation of Power Transferred through the Phases of L-L-L fault in Six Phase Mode

For a L-L-L fault on Phases a, f and e at a point P, close to the sending end bus of the line in six phase single circuit mode, only the faulted phases have been modelled as in Figure 4.4.

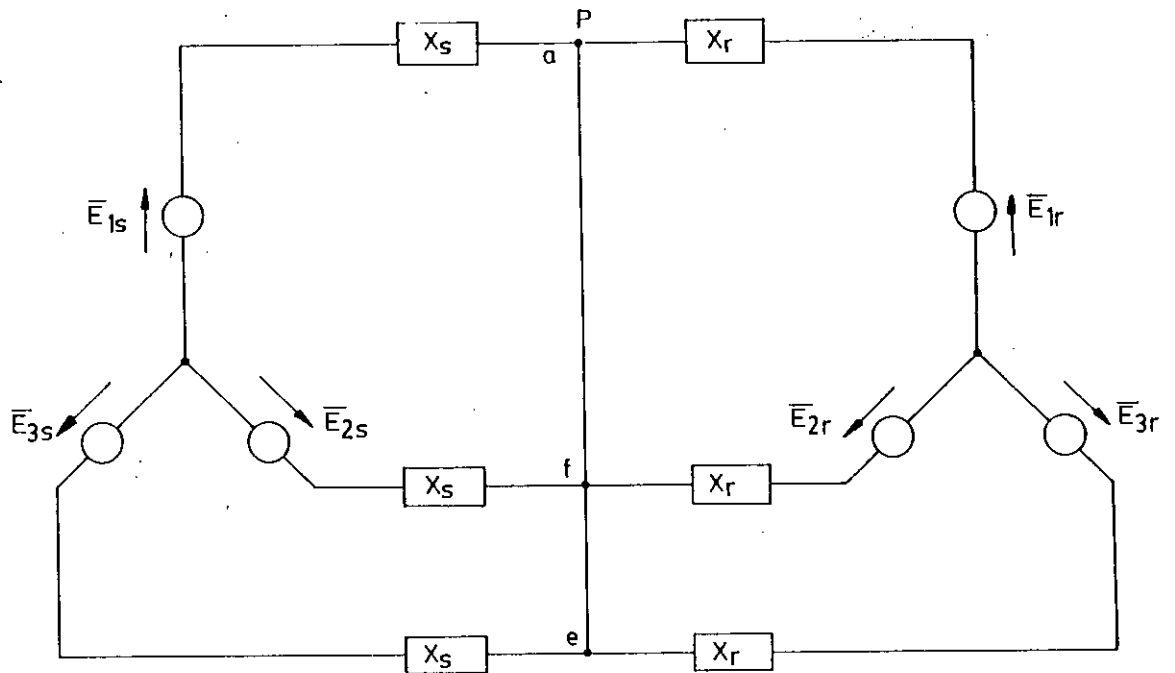


Figure 4.4: Modelling of a L-L-L fault on six phase single circuit line.

Each of the three emf sources along with respective reactance in series on either side of the fault point P, can be converted into a current source with a parallel conductance (reciprocal of the corresponding reactance) as shown in Figure 4.5 .

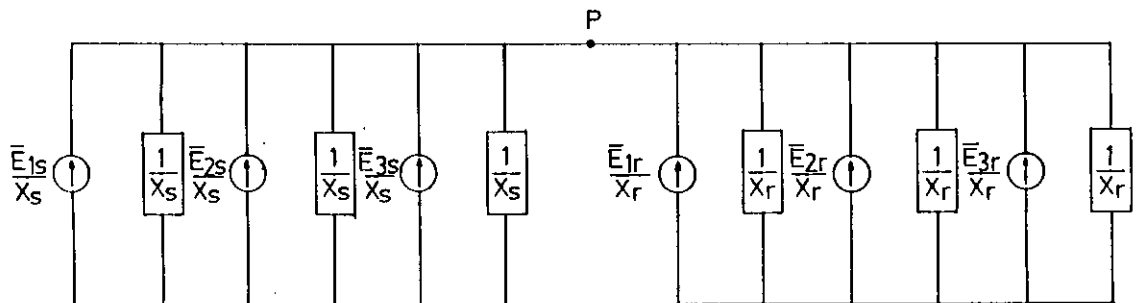


Figure 4.5: Conversion of emf sources of Figure 4.4 into current sources.

The three current sources together with their parallel conductances on either side of the fault point P can be reconverted into a single emf source with a combined reactance in series as in Figure 4.6.

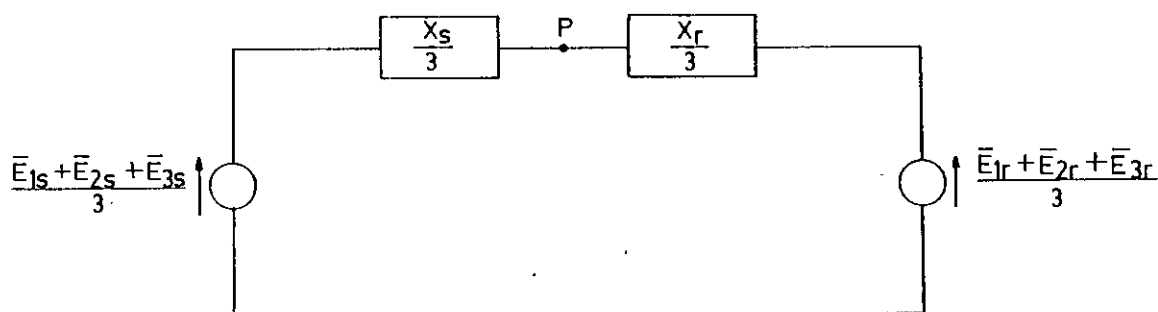


Figure 4.6: Simplification of model of Figure 4.5 by reconversion of current sources into emf sources.

The maximum power transferability P_f through the three faulted phases (a-f-e) can be computed by equation (4.8).

$$P_f = \frac{(\bar{E}_{1s} + \bar{E}_{2s} + \bar{E}_{3s}) * (\bar{E}_{1r} + \bar{E}_{2r} + \bar{E}_{3r})}{3(X_s + X_r)} \quad (4.8)$$

The maximum total power transferability P_{maxd} for the L-L-L fault is then calculated by adding P_f to the total of the limits obtained from equation (4.6) applied to each of the three unfaulted phases b, c and d.

4.5 Determination of Postfault Limit

It has been considered in the present work that the faults are cleared by three pole breaking at both ends of the line, as is the practice⁹. This means that for any selected fault on one of the two circuits in the three phase mode, all the three conductors of the affected circuit are taken out. Similarly to clear any selected fault in six phase mode, the conductors of one side are taken out. Based on this consideration, the maximum total postfault power transferability P_{max} has been determined by adding together each of the limits obtained from equation (4.6) applied to each phase of the unfaulted circuit or side in 3- ϕ or 6- ϕ modes.

4.6 Results on Critical Clearing Angles

Table 4.2 shows the critical clearing angles, determined through the application of equation (4.1) in the way mentioned in sections 4.2 to 4.5, for each of the selected fault types (specified in Table 3.1).

It is worth-mentioning that the angles δ_0 and δ_{max} as in equations (4.2) and (4.3) were computed considering both P_m and P_{max} on per phase basis.

It should be noted that for a number of faults in the three modes, the critical clearing angle was indeterminate such that its cosine value was outside the range ± 1 . In Table 4.2 these cases have been referred to as inherently stable (I.S.) or stable for sustained⁹ fault condition i.e. transient stability is not lost even if those faults are not cleared. In inherently stable cases, the

Table 4.2: Critical clearing angles in three modes of the line for fault at the sending end

Type of fault	132 KV three phase double circuit						230 KV three phase double circuit					132 KV six phase single circuit					
	faulted phases	P_m p.u./ phase	P_{max} p.u./ phase	r_1	r_2	δ_{cr} (elect. degrees)	P_m p.u./ phase	P_{max} p.u./ phase	r_1	r_2	δ_{cr} (elect. degrees)	faulted phases	P_m p.u./ phase	P_{max} p.u./ phase	r_1	r_2	δ_{cr} (elect. degrees)
L-G	a-g	1.0	2.81	0.666	0.583	I.S	1.0	4.06	0.666	0.744	I.S	a-g	1.0	3.04	0.833	0.5	I.S
L-L	a-b	1.0	2.81	0.5	0.583	I.S	1.0	4.06	0.5	0.744	I.S	i)a-e ii)a-f	1.0 1.0	3.04 3.04	0.75 0.75	0.5 0.5	I.S I.S
L-L-G	a-b-g	1.0	2.81	0.333	0.583	94.14	1.0	4.06	0.333	0.744	164.2	i)a-e-g ii)a-f-g	1.0 1.0	3.04 3.04	0.666 0.666	0.5 0.5	I.S I.S
L-L-L	a-b-c	1.0	2.81	0.0	0.583	59.83	1.0	4.06	0.0	0.744	95.61	a-f-e	1.0	3.04	0.723	0.5	I.S
L-L-L-G		same as L-L-L					Same as L-L-L					a-f-e-g	1.0	3.04	0.5	0.5	I.S

Legend : I.S : inherently stable

maximum electrical power transferred during the fault was sufficiently above the prime mover input so that a retarding force acted to prevent loss of synchronism and hence stability.

4.7 Conclusions

The transient has been determined in terms of critical clearing angle using a common formula for all the practical faults in three and six phase modes of the line under study. The way this formula has been applied is simple and new. In this technique the ratios of during-fault to pre-fault and post-fault to pre-fault power transferability limits have been computed using the total of the individual limits on power transferable through each of the faulted as well as unfaulted phases. The fact that some power is transferred through the faulted phases during a two-phase (L-L) fault in both three and six phase modes and during a three-phase (L-L-L) fault only in six phase mode, has been taken into account through a simple and new modelling technique.

A comparison of the critical clearing angles for the three modes shows that the six phase single circuit system is the most stable one for all the types of faults considered at the worst location. In increasing order of stability the three systems can be arranged as : 132 KV 3- ϕ , 230 KV 3- ϕ and 132 KV 6- ϕ .

CHAPTER 5
CONCLUSIONS

5.1 Conclusions

In the present research work a comprehensive study has been made regarding power transferability, configurational safety factor, system fault level and transient stability of a line in 132 KV six phase single circuit mode and compared with those in the 132 KV and 230 KV three phase double circuit modes. The Ghorasal-Ishurdi line of Bangladesh Power Development Board grid system was considered for the study.

The three phase network at each end of the line was modelled as a Thevenin's emf in series with a reactance. The model proposed for the phase conversion transformer required in six phase mode of the line, was simple and easy-to-implement.

The fault and the transient stability analyses have been done in the three modes for practical faults (both balanced and unbalanced) which involved the physically adjacent conductors. Simple techniques on a unified basis were used for those analyses in the three modes. These techniques did not require complexities of the symmetrical component method. The fault currents were determined applying the loop current method.

The transient stability was quantified in terms of critical clearing angles. These angles were obtained in the three modes using the same formula derived from the principle of equal area criterion. The formula for critical clearing angle needed computation of power transferabilities before, during and after fault. The equation for per phase power transferability of a balanced network before fault, has also been applied for each unfaulted phase of the network during

and after fault conditions. For two-phase (L-L) faults in both three and six phase modes and three-phase fault (L-L-L) in six phase mode, the power transferability during fault through the affected phases has been determined using a new method. In this method the faulted phases were modelled such that they eventually resulted in only two emf sources, at two sides of the fault point, being connected by a delta network. The two ratios: (1) limit of power transferability during fault to pre-fault limit of power transferability and (2) post fault limit to pre-fault limit, were determined using total of the limits for each of the faulted and unfaulted phases. This method of calculating the two ratios was able to consider in an easy way, the effects of both balanced and unbalanced faults in the formula used for critical clearing angle.

The following are some of the salient findings of the present investigation.

- 1) The conversion of existing 132 KV three phase double circuit line into a 132 KV six phase single circuit line, using the same rights-of-way, will have practically insignificant effects on safety margins regarding ground clearance and inter conductor spacings.
- 2) The steady-state power transferabilities (proportional to the square of line to neutral voltage) for the 230 KV three phase double circuit line and the 132 KV six phase single circuit line, both are almost three times higher than that of the 132 KV three phase single circuit line. However if the thermal loadability limit is considered, the power transferability through the 132 KV six phase line is 1.73 times that in 132 KV three phase mode and is only about 14% less than

that of the 230 KV three phase line. But 230 KV 3- ϕ line like the one studied by the present work, may require use of bigger sized conductors with higher current carrying capacity and also a new tower in a wider corridor incurring more cost than that of converting an existing 132 KV three phase line into a 132 KV six phase one.

3) For the same type and location of fault, the six phase line was found to have the least fault level. The three-phase to ground fault on the line close to the sending end was the severest fault and in this case the fault level of the line in 132 KV six phase mode was about 62% and 92% respectively of those in the 132 KV three phase and 230 KV three phase modes. This implies also a proportionate decrease in size of the switchgear components necessary for the six phase line. The decrease in fault level of six phase line mainly stems from the increased line reactance.

4) For all the types of faults considered at the worst location, the six phase line was found the most stable one even if the faults are not cleared. The increase in stability of six phase line mainly results from increased number of phases permitting more power transferability.

5.2 Suggestions for Future Research

The following are some of the potential areas being suggested for future research.

1) An investigation can be made to conduct a load flow analysis considering all the phases of the three phase network and the six phase lines embeded in it simultaneously, by forming a loop

impedance matrix based on the modelling proposed in the present research work.

2) An experimental prototype can be developed for a typical power system network comprising normal three phase lines and one or more six phase transmission lines, to carry out fault and stability analysis simulating the practical faults considered by the present work.

3) A protective relaying scheme can be designed based on the results obtained in the present investigation and tested on the above mentioned prototype.

REFERENCES

1. N.B. BHATT, S.S. VENKATA, W.C. GUYKER and W.H. BOOTH: "Six-phase (multi-phase) Power Transmission Systems: Fault Analysis", IEEE Transactions on Power Apparatus and Systems. Vol. PAS-96, No. 3, May/June 1977, pp. 758-767.
2. S.S. VENKATA, W.C. GUYKER, J. KONDRAGUNTA, N.K. SAINI and E.K. STANEK: "138 KV, Six-phase Transmission Systems: Fault Analysis", IEEE Transaction on Power Apparatus and Systems, Vol. PAS-101, No. 5, MAY 1982, pp. 1203-1218.
3. S.N. TIWARI and L.P. SINGH: "Mathematical Modelling and Analysis of Multi Phase Systems", IEEE Transactions on Power Apparatus and Systems, Vol. PAS-101, No. 6, June 1982, pp. 1784-1793.
4. A. CHANDRASEKARAN, S. ELANGOVAN and P.S. SUBRAHANIAN: "Stability Aspect of a Six Phase Transmission System:", IEEE Transactions on Power Systems, Vol. PWRs-1, No. 1, February 1986, pp. 108-112.
5. B.K. BHAT and R.D. SHARMA: "Analysis of Simultaneous Ground and Phase Faults on a Six Phase Power Systems", IEEE Transactions on Power Delivery, Vol. 4, No. 3, July 1989, pp. 1601-1616.
6. E.H. BADAWY, M.K. EL-SHERBINY, A.A. IBRAHIM and M.S. FARGHALY: "A Method of Analyzing Unsymmetrical Faults on Six Phase Power Systems", 90WM 081-0 PWRD: preprint of a paper recommended and approved by the IEEE Transmission and Distribution Committee of the IEEE Power Engineering Society for presentation at the IEEE/PES 1990 Winter Meeting,

Atlanta, Georgia, February 4-8, 1990.

7. A.E. GUILLE and W. PATERSON: "Electrical Power Systems", Volume 1, 1982, Pergamon Press, Oxford, UK; pp. 307-309.
8. R.M. KERCHNER and G.F. CORCORAN: "Alternating Current Circuits", Fourth Edition, 1960, John Wiley and Sons, Inc., Japan. pp. 336-337, 377-378, 546.
9. W.D. STEVENSON, Jr.: "Elements of Power System Analysis", McGraw-Hill Book Company, Singapore. Third Edition, 1985, pp. 145-148, Fourth Edition, 1986, pp. 50-61, 107-110, 393-400.
10. E.W. KIMBARK: "Power System Stability", Volume 1, 1962, John Wiley and Sons, Inc., New York. pp. 127-130.

APPENDIX A
DERIVATION OF THE EXPRESSION FOR
STEADY STATE POWER
TRANSFERABILITY

A.1 Derivation of Equation (2.5)

The maximum limit of the steady-state power transferable to the receiving end of a transmission line has been derived from a π circuit representation^a of the line on per phase basis shown in Figure A.1 .

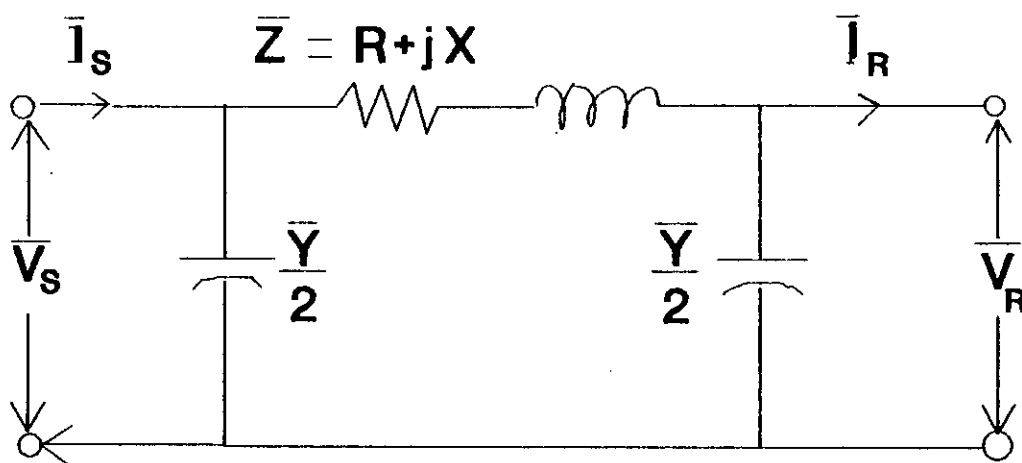


Figure A.1: Representation of one phase of a transmission line through π - model.

The various symbols used in Figure A.1 have the following significance.

\bar{V}_s = Sending end phase to neutral voltage phasor.

\bar{V}_R = Receiving end phase to neutral voltage phasor.

\bar{I}_s = Sending end current phasor.

\bar{I}_R = Receiving end current phasor.

$\bar{Z} = R + jX$ (A.1)

is the total series impedance of the line per phase.

\bar{Y} = total line susceptance due to charging capacitance.

It follows from Figure A.1 that \bar{V}_S can be written as in equation (A.2).

$$\bar{V}_S = (\bar{I}_R + \bar{V}_R \frac{\bar{Y}}{2}) \bar{Z} + \bar{V}_R \quad (\text{A.2})$$

Solving equation (A.2) for \bar{I}_R provides equation (A.3).

$$\bar{I}_R = \frac{\bar{V}_S - (1 + \bar{Z} \frac{\bar{Y}}{2}) \bar{V}_R}{\bar{Z}} \quad (\text{A.3})$$

For the sake of simplicity in symbolism, the phasors \bar{V}_R , \bar{V}_S , \bar{Z} and $(1 + \bar{Z} \frac{\bar{Y}}{2})$ have been redesignated as in equation (A.4) to (A.7) respectively.

$$\bar{V}_R = V_R \angle 0 \quad (\text{A.4})$$

$$\bar{V}_S = V_S \angle \delta \quad (\text{A.5})$$

$$\bar{B} = \bar{Z} \quad (\text{A.6})$$

$$\bar{A} = 1 + \bar{Z} \frac{\bar{Y}}{2} \quad (\text{A.7})$$

Substituting equations (A.7) and (A.6) respectively for $(1 + \bar{Z} \frac{\bar{Y}}{2})$ and \bar{Z} in equation (A.3) provides equation (A.8).

$$\bar{I}_R = \frac{\bar{V}_S - \bar{A} \bar{V}_R}{\bar{B}} \quad (\text{A.8})$$

The phasors \bar{A} and \bar{B} can also be written in polar form as in equation (A.9) and (A.10) respectively.

$$\bar{A} = A \angle \alpha \quad (\text{A.9})$$

$$\bar{B} = B \angle \beta \quad (\text{A.10})$$

Combining equations (A.4), (A.5), (A.8), (A.9) and (A.10), \bar{I}_R can be obtained as in equation (A.11).

$$\bar{I}_R = \frac{V_S}{B} \angle (\delta - \beta) - \frac{AV_R}{B} \angle (\alpha - \beta) \quad (\text{A.11})$$

The power at the receiving end is equal to the real part of the complex quantity $\bar{V}_R \bar{I}_R^*$ as in equation (A.12).

$$P = \frac{V_S V_R}{B} \cos(\beta - \delta) - \frac{AV_R^2}{B} \cos(\beta - \alpha) \quad (\text{A.12})$$

It follows from equation (A.12) that power at the receiving end will be maximum for $(\beta - \delta)$ equal to zero and the expression of this maximum power is as in equation (A.13)

$$P_{\max} = \frac{V_S V_R}{B} - \frac{AV_R^2}{B} \cos(\beta - \alpha) \quad (\text{A.13})$$

If the series resistance R of the line is neglected then equations (A.1), (A.6) and (A.10) provides equation (A.14).

$$\bar{B} = X \angle 90^\circ \quad (\text{A.14})$$

If the shunt capacitances of the line are also neglected then equations (A.7) and (A.9) provides equation (A.15).

$$\bar{A} = 1 \angle 0^\circ \quad (\text{A.15})$$

It follows from equations (A.14) and (A.15) that β and α are respectively 90° and 0° so that $(\beta - \alpha)$ is equal to 90° . Then substituting equations (A.14) and (A.15) into equation (A.13) provides P_{\max} as in equation (A.16) which is same as equation (2.5).

$$P_{\max} = \frac{V_S V_R}{X} \quad (\text{A.16})$$

APPENDIX B
DERIVATION OF THE EXPRESSION FOR
LINE INDUCTANCE

B.1 Determination of Average Inductance Per Conductor

The average inductance of one conductor of a multiphase single or double circuit transmission line, assumed to be transposed, can be obtained after determining its flux linkages corresponding to each position it occupies in the transposition cycle.

The transposition cycle of a group of six conductors, e.g. a three phase double circuit line or a six phase single circuit line, has been shown in Figure B.1.

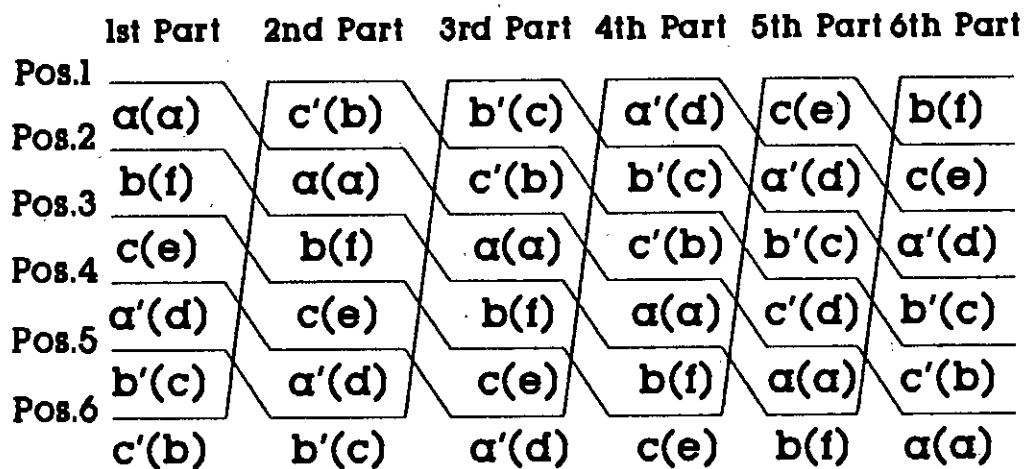


Figure B.1: A complete transposition cycle of a three phase double circuit or a six phase single circuit transmission line.

In Figure B.1 the symbols inside the parentheses i.e. α, f, e, b, c, d denote the conductors of respective phases in the two sides of the six phase single circuit line. On the otherhand, the

symbols without bracket i.e. a, b, c, a', b', c' denote the conductors of the respective phases in the two circuits of the three phase double circuit line and it should be noted that the conductors (a, a'), (b, b') and (c, c') are in parallel forming the phases a, b and c respectively.

The phasor expression for the flux linkage of conductor a in 1st part of the transposition cycle i.e. when a is in position 1, b in position 2, c in position 3, a' in position 4, b' in position 5 and c' in position 6, is given^o by equation (B.1).

$$\bar{\Psi}_{a1} = 2 \times 10^{-7} \left(\bar{I}_a \ln \frac{1}{D_s} + \bar{I}_b \ln \frac{1}{D_{12}} + \bar{I}_c \ln \frac{1}{D_{13}} + \bar{I}_{a'} \ln \frac{1}{D_{14}} + \bar{I}_{b'} \ln \frac{1}{D_{15}} + \bar{I}_{c'} \ln \frac{1}{D_{61}} \right) \quad (\text{B.1})$$

Similarly in 2nd to 6th parts of the cycle the flux linkages of conductor a are respectively as in equations (B.2) to (B.6).

$$\bar{\Psi}_{a2} = 2 \times 10^{-7} \left(\bar{I}_a \ln \frac{1}{D_s} + \bar{I}_b \ln \frac{1}{D_{23}} + \bar{I}_c \ln \frac{1}{D_{24}} + \bar{I}_{a'} \ln \frac{1}{D_{25}} + \bar{I}_{b'} \ln \frac{1}{D_{26}} + \bar{I}_{c'} \ln \frac{1}{D_{12}} \right) \quad (\text{B.2})$$

$$\bar{\Psi}_{a3} = 2 \times 10^{-7} \left(\bar{I}_a \ln \frac{1}{D_s} + \bar{I}_b \ln \frac{1}{D_{34}} + \bar{I}_c \ln \frac{1}{D_{35}} + \bar{I}_{a'} \ln \frac{1}{D_{36}} + \bar{I}_{b'} \ln \frac{1}{D_{13}} + \bar{I}_{c'} \ln \frac{1}{D_{23}} \right) \quad (\text{B.3})$$

$$\bar{\Psi}_{a4} = 2 \times 10^{-7} \left(\bar{I}_a \ln \frac{1}{D_s} + \bar{I}_b \ln \frac{1}{D_{45}} + \bar{I}_c \ln \frac{1}{D_{46}} + \bar{I}_{a'} \ln \frac{1}{D_{14}} + \bar{I}_{b'} \ln \frac{1}{D_{24}} + \bar{I}_{c'} \ln \frac{1}{D_{34}} \right) \quad (\text{B.4})$$

$$\bar{\Psi}_{a5} = 2 \times 10^{-7} \left(\bar{I}_a \ln \frac{1}{D_s} + \bar{I}_b \ln \frac{1}{D_{56}} + \bar{I}_c \ln \frac{1}{D_{15}} + \bar{I}_{a'} \ln \frac{1}{D_{25}} + \bar{I}_{b'} \ln \frac{1}{D_{35}} + \bar{I}_{c'} \ln \frac{1}{D_{45}} \right) \quad (\text{B.5})$$

$$\bar{\Psi}_{a6} = 2 \times 10^{-7} \left(\bar{I}_a \ln \frac{1}{D_s} + \bar{I}_b \ln \frac{1}{D_{61}} + \bar{I}_c \ln \frac{1}{D_{26}} + \bar{I}_{a'} \ln \frac{1}{D_{36}} + \bar{I}_{b'} \ln \frac{1}{D_{46}} + \bar{I}_{c'} \ln \frac{1}{D_{56}} \right) \quad (\text{B.6})$$

The average value of the flux linkage of conductor a is in

equation (B.7).

$$\bar{\Psi}_a = \frac{\bar{\Psi}_{a1} + \bar{\Psi}_{a2} + \bar{\Psi}_{a3} + \bar{\Psi}_{a4} + \bar{\Psi}_{a5} + \bar{\Psi}_{a6}}{6} \quad (\text{B.7})$$

Combining equations (B.1) to (B.7) $\bar{\Psi}_a$ can be obtained as in equation (B.8).

$$\bar{\Psi}_a = \frac{2 \times 10^{-7}}{6} \left(6\bar{I}_a \ln \frac{1}{D_s} + \bar{I}_b \ln \frac{1}{D_1} + \bar{I}_c \ln \frac{1}{D_2} + \bar{I}_a' \ln \frac{1}{D_3} + \bar{I}_b' \ln \frac{1}{D_2} + \bar{I}_c' \ln \frac{1}{D_1} \right) \quad (\text{B.8})$$

where,

D_s = GMR (Geometric mean radius) of the conductor

$$D_1 = D_{12}D_{23}D_{34}D_{45}D_{56}D_{61} \quad (\text{B.9})$$

$$D_2 = D_{13}D_{24}D_{35}D_{46}D_{15}D_{26} \quad (\text{B.10})$$

$$D_3 = (D_{14}D_{25}D_{36})^2 \quad (\text{B.11})$$

D_{12} = Distance between positions 1 and 2 and similar significance for D_{23} , D_{34} etc.

B.1.1 Inductance of Three Phase Line

Since for a balanced three phase double circuit line $\bar{I}_a = \bar{I}_a'$, $\bar{I}_b = \bar{I}_b'$ and $\bar{I}_c = \bar{I}_c'$ equation (B.8) can be re-written as in equation (B.12).

$$\bar{\Psi}_a = 2 \times 10^{-7} \left(\bar{I}_a \ln \frac{1}{D_s D_3^{\frac{1}{6}}} + \bar{I}_b \ln \frac{1}{D_1^{\frac{1}{6}} D_2^{\frac{1}{6}}} + \bar{I}_c \ln \frac{1}{D_1^{\frac{1}{6}} D_2^{\frac{1}{6}}} \right) \quad (\text{B.12})$$

As the phasor sum of three balanced currents in a three phase system is zero, it follows that

$$\bar{I}_b + \bar{I}_c = -\bar{I}_a \quad (\text{B.13})$$

Combining equation (B.12) and (B.13) $\bar{\Psi}_a$ can be expressed as in equation (B.14).

$$\bar{\Psi}_a = 2 \times 10^{-7} \bar{I}_a \ln \left(\frac{\sqrt[6]{D_1 D_2}}{D_s \sqrt[6]{D_3}} \right) \quad (\text{B.14})$$

Then the average inductance L_a (Henry/meter) per conductor per phase of the three phase double circuit line is $\frac{\bar{\Psi}_a}{\bar{I}_a}$ and as in equation (B.15).

$$L_a = 2 \times 10^{-7} \ln \left(\frac{\sqrt[6]{D_1 D_2}}{D_s \sqrt[6]{D_3}} \right) \quad (\text{B.15})$$

B.1.2 Inductance of Six Phase Line

The equation (B.8) can also be extended for determining the average flux linkage of a conductor in the six phase line. For this the phasors \bar{I}_b , \bar{I}_c , \bar{I}_a' , \bar{I}_b' and \bar{I}_c' are to be replaced respectively by \bar{I}_f , \bar{I}_e , \bar{I}_d , \bar{I}_c and \bar{I}_b in equation (B.8). This results in equation (B.16).

$$\bar{\Psi}_a = \frac{2 \times 10^{-7}}{6} \left(6 \bar{I}_a \ln \frac{1}{D_s} + \bar{I}_f \ln \frac{1}{D_1} + \bar{I}_e \ln \frac{1}{D_2} + \bar{I}_d \ln \frac{1}{D_3} + \bar{I}_c \ln \frac{1}{D_2} + \bar{I}_b \ln \frac{1}{D_1} \right) \quad (\text{B.16})$$

Since for a balanced six phase single circuit line $\bar{I}_d = -\bar{I}_a$, $\bar{I}_f = -\bar{I}_e$ and $\bar{I}_b = -\bar{I}_c$ (based on Figure 2.1(b) in section 2.3.1) equation (B.16) can be written as in equation (B.17).

$$\bar{\Psi}_a = \frac{2 \times 10^{-7}}{6} \left(\bar{I}_a \ln \frac{D_3^{\frac{1}{6}}}{D_s} + \bar{I}_c \ln \frac{D_1^{\frac{1}{6}}}{D_2^{\frac{1}{6}}} + \bar{I}_e \ln \frac{D_1^{\frac{1}{6}}}{D_2^{\frac{1}{6}}} \right) \quad (\text{B.17})$$

As the phasors \bar{I}_a , \bar{I}_c and \bar{I}_e are 120° displaced from each other in a balanced six phase system (based on Figure 2.1(b) in section 2.3.1) it follows that

$$\bar{I}_c + \bar{I}_e = -\bar{I}_a \quad (\text{B.18})$$

Combining equations (B.17) and (B.18), $\bar{\Psi}_a$ can be expressed as in equation (B.19).

$$\bar{\Psi}_a = 2 \times 10^{-7} \bar{I}_a \ln \left(\frac{\sqrt[6]{D_2 D_3}}{D_s \sqrt[6]{D_1}} \right) \quad (\text{B.19})$$

Then the average inductance L_a (Henry/meter) per phase of the six phase single circuit line is $\frac{\bar{\Psi}_a}{\bar{I}_a}$ and as in equation (B.20).

$$L_a = 2 \times 10^{-7} \ln \left(\frac{\sqrt[6]{D_2 D_3}}{D_s \sqrt[6]{D_1}} \right) \quad (\text{B.20})$$

APPENDIX C
DERIVATION OF THE EXPRESSION FOR
CRITICAL CLEARING ANGLE

C.1 Critical Clearing Angle From Equal Area Criterion

The swing, δ , of the rotor of a synchronous machine with respect to an infinite bus or another synchronous machine to which it is connected through a transmission line can be expressed as in equation (C.1).

$$M \frac{d^2\delta}{dt^2} = P_m - P_e \quad (C.1)$$

where,

M = Inertia constant of the machine.

P_m = constant mechanical power delivered from the prime mover of the machine.

P_e = Developed electrical power of the synchronous machine equal to that which can be transferred from sending end to the receiving end of the line at a swing value of δ .

The developed power (P_e) versus swing (δ) curve^a for the machine in prefault condition i.e. prior to occurrence of any fault on the line, has been shown in Figure C.1.

In Figure C.1 the angle δ_0 is the initial value of the machine's swing when its developed electrical power was equal to the prime mover output P_m . As a result the machine was at synchronous speed at the value δ_0 .

If a fault occurs on the line between two machines such that some power (less than that in prefault condition) is transferred from the sending end to the receiving end, then the developed electrical

power decreases as shown in Figure C.1 and the balance between input from the primemover and electric power output of the sending end machine is disturbed. As a result the machine's rotor speed accelerates and increases above the synchronous speed. At the same time the rotor swing goes on advancing beyond δ_0 .

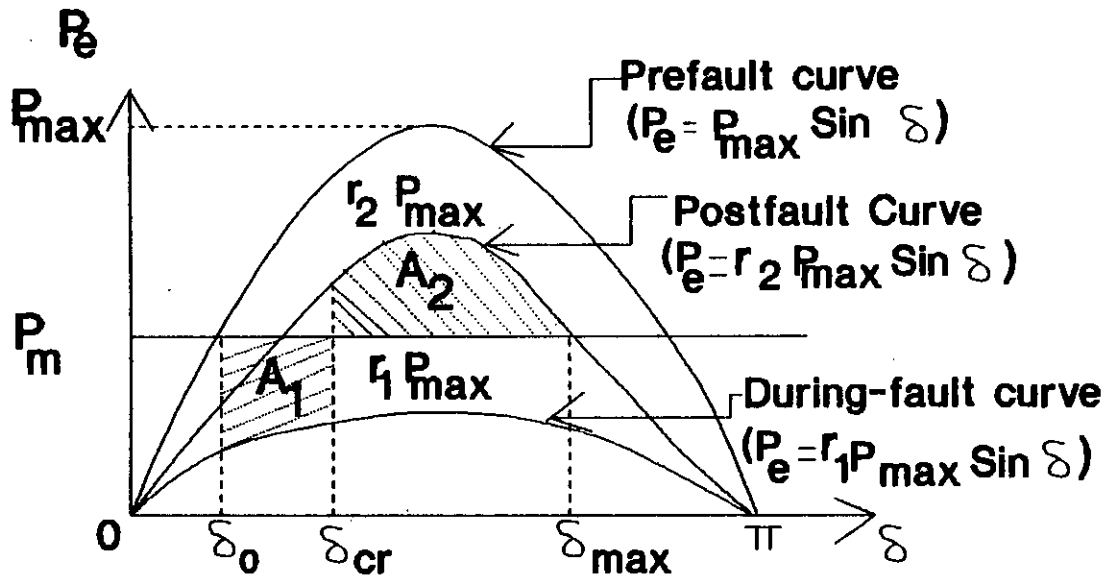


Figure C.1: Developed electrical power versus swing curve of a synchronous machine.

In order that the machine's speed can be restored back to the synchronous value, the fault must be cleared at or before a swing value, termed critical clearing angle δ_{cr} .

If the fault is cleared at or before δ_{cr} the developed or output electrical power curve is as shown in Figure C.1. It should be noted, as in Figure C.1, that after clearing the fault, the electric power output abruptly rises to a new value and the machine's rotor speed will decelerate. It can be restored back to the synchronous speed and hence a stable operation, provided the rotor swing has not advanced

beyond the maximum limit δ_{max} at which the electrical power output P_e again balances the primemover output P_m .

Mathematically the swing and restoration phenomena can be related to the fact that whatever kinetic energy was added to the rotor while it was accelerating (from δ_0 to δ_{cr}) after the occurrence of a fault, must be released while it is decelerating (from δ_{cr} to δ_{max}) after clearing the fault.

Since kinetic energy is $\frac{1}{2}M\omega^2$ and $\omega = \frac{d\delta}{dt}$ is the angular velocity relative to the synchronous speed it can be written that

$$K.E = \frac{1}{2}M \frac{d\delta}{dt}^2 \quad (C.2)$$

Multiplying both sides of equation (C.1) by $\frac{d\delta}{dt}$ provides equation (C.3)

$$M \frac{d^2\delta}{dt^2} \frac{d\delta}{dt} = (P_m - P_e) \frac{d\delta}{dt} \quad (C.3)$$

$$\text{or, } \frac{1}{2}M \frac{d}{dt} \left(\frac{d\delta}{dt} \right)^2 = (P_m - P_e) \frac{d\delta}{dt} \quad (C.4)$$

Multiplying both sides of equation (C.4) by dt and integrating between two limits of swing angle δ_1 and δ_2 provides equation (C.5).

$$\frac{1}{2}M \left(\frac{d\delta}{dt} \right)^2 = \int_{\delta_1}^{\delta_2} (P_m - P_e) d\delta \quad (C.5)$$

$$\text{or, } \frac{d\delta}{dt} = \sqrt{\frac{2}{M} \int_{\delta_1}^{\delta_2} (P_m - P_e) d\delta} \quad (C.6)$$

Combining equation (C.2) and (C.6) gives

$$K.E = \sqrt{\frac{M}{2}} \sqrt{\int_{\delta_1}^{\delta_2} (P_m - P_o) d\delta} \quad (C.7)$$

Application of equation (C.7) to the power-swing curve in Figure B.1 shows that the kinetic energy added to the rotor is proportional to the area A_1 and the kinetic energy released from the rotor is proportional to the area A_2 . Therefore for restoration of the synchronous speed, these two area, must be equal as in equation (C.8)

$$A_1 = A_2 \quad (C.8)$$

$$\text{or, } \int_{\delta_o}^{\delta_{cr}} (P_m - r_1 P_{max} \sin\delta) d\delta = \int_{\delta_{cr}}^{\delta_{max}} (r_2 P_{max} \sin\delta - P_m) d\delta \quad (C.9)$$

$$\text{or, } P_m(\delta_{cr} - \delta_o) + r_1 P_{max} (\cos\delta_{cr} - \cos\delta_o) = r_2 P_{max} (\cos\delta_{cr} - \cos\delta_{max}) - P_m(\delta_{max} - \delta_{cr}) \quad (C.10)$$

$$\text{or, } (r_1 - r_2) P_{max} \cos\delta_{cr} = P_m(\delta_o - \delta_{max}) - r_2 P_{max} \cos\delta_{max} - r_1 P_{max} \cos\delta_o \quad (C.11)$$

$$\text{or, } \cos\delta_{cr} = \frac{\frac{P_m}{P_{max}}(\delta_{max} - \delta_o) + r_2 \cos\delta_{max} - r_1 \cos\delta_o}{r_2 - r_1} \quad (C.12)$$

$$\text{or, } \delta_{cr} = \cos^{-1} \left[\frac{\frac{P_m}{P_{max}}(\delta_{max} - \delta_o) + r_2 \cos\delta_{max} - r_1 \cos\delta_o}{r_2 - r_1} \right] \quad (C.13)$$

Equation (C.13) is the same as equation (4.1).

